Use Authorization

In presenting this thesis in partial fulfillment of the requirements for an advanced degree at Idaho State University, I agree that the Library shall make it freely available for inspection. I further state that permission to download and/or print my thesis for scholarly purposes may be granted by the Dean of the Graduate School, Dean of my academic division, or by the University Librarian. It is understood that any copying or publication of this thesis for financial gain shall not be allowed without my written permission.

Signature_____

Date _____

EFFECTS OF MUTATIONS IN THE C-LOOP OF α3β2- NICOTINIC ACETYLCHOLINE RECEPTOR ON LIGAND BINDING

by

Jingijng Li

A thesis

Submitted in partial fulfillment

Of the requirement for the degree of

Master of Science in the Department of Biological Sciences

Idaho State University

Summer 2017

Committee Approval

To the Graduate Faculty:

The members of the committee appointed to examine the thesis of Jingjing Li find it satisfactory and recommend that it be accepted.

_____

James R. Groome, PhD. Major Advisor

_____

Kenneth Rodnick, PhD. Committee Member

_____

Michele R. Brumley, PhD. Graduate Faculty Representative

DEDICATION

This thesis is dedicated for my family and friends. This would not have been possible without their support and unconditional love.

ACKNOWLEDGMENTS

First, I want to express my gratitude to my advisor, Dr. James Groome, who introduced me into the world of electrophysiology and spent tremendous effort in keeping me on the right track to successfully completing this project. I'm grateful for all the time he spent on explaining different concepts, helping me with the techniques of two-electrode voltage clamp. I have learned much more than just scientific knowledge, but more importantly, the attitude of doing science.

I would like to acknowledge my committee member, Dr. Kenneth Rodnick, for providing huge support on MOE software and giving me the opportunity to appreciate different data analytic methods.

I also want to thank my lab mate, Rosey Whiting, who helped me hugely when I first started working in the lab. She was a great source of lab equipment, frog care and other necessities. Jordan Broadway, was a good company in the lab and in the frog room. Rachel Kruger and Matt Seaman, who have also contributed to the data for this thesis. Landon Edwards, Ryann Camp and Kshitij Shrestha, who helped me in other necessities.

I thank the Biological Department of Idaho State University for providing the teaching assistantship and a great experience for this M.S. I have gained so much from this program.

TABLE OF CONTENTS

LIST OF FIGURES

LIST OF TABLES

LIST OF ABBREVIATIONS

Ach: Acetylcholine

Ac-nAchBP: *Aplysia californic*a nicotinic acetylcholine binding protein

ANS: Autonomic nervous system

cDNA: complementary DNA

CNS: Central nervous system

DA: Dopamine

EC_{50}: The excitatory concentration that produce half-maximal response

mAchR(s): Muscarinic acetylcholine receptor(s)

MD: Molecular dynamics

MOE (molecular operating environment): the software that was used for docking experiments

mRNA: Messenger RNA

nAchR(s): Nicotinic acetylcholine receptor(s)

PD: Parkinson's disease

PNS: Peripheral nervous system

SN: Substantia nigra

TEVC: Two-electrode voltage clamp

VTA: Ventral tegmental area

WT: wild type

ABSTRACT

Nicotinic acetylcholine receptors (nAchRs) belong to the Cys-loop (C-loop) ligand-gated ion channel superfamily, and each receptor consists of five different subunits as a heteropentamer. Ach or other agonist binding promotes the opening of the ion channel to allow ions to pass through, and these receptor channels have been found in both the central nervous system (CNS) and peripheral nervous system (PNS) (Tritsch et al., 2014). The composition of nAchR subunits determines their subtype, which determines the nAchRs' pharmacological characteristics and locations. Their regulation of dopaminergic neurons in the nigrostriatal dopaminergic pathway are important in understanding the symptoms observed in Parkinson's disease, and they play a role in other diseases, such as Sudden Infant Death Syndrome and Alzheimer's disease. The study of nAchRs is critical to the development of pharmacological approaches to treat these diseases (Sambasivarao et al., 2013).

The purpose of this study is to investigate ligand binding of the α3β2 nAchR, by determining the effects of specific mutations in the C-loop of the binding pocket in both α3-β2 and β2-α3 interfaces for Ach and α-conotoxin MII binding. Previous studies suggest that the nAchR agonist binding site is under the C-loop, promoting the hypothesis that the flexibility of the C-loop directly affects the binding efficiency of the nAchR. Two-electrode voltage clamp electrophysiology was used to study *Xenopus* oocytes expressing wild type and mutant nAchRs. Homology modeling and MOE simulations were also used to complement the two-electrode voltage clamp experiments to understand effects of the mutations for Ach binding and α-conotoxin MII binding. The

results showed the mutations of interest have more effect on α-conotoxin MII binding than Ach binding.

INTRODUCTION

Acetylcholine as A neurotransmitter and neuromodulator

For a long time, it has been known that body movements are carried out by skeletal muscles, but there was little known about what neurochemical transmitter activates muscles. It turned out to be acetylcholine, as a neurotransmitter that is released from motor neurons at the neuromuscular junction, to stimulate muscle movement. Acetylcholine (Ach), is an organic chemical compound that is named after its chemical structure, an ester of acetic acid and choline. It is produced by cholinergic neurons and has important functions both in the brain and body as neurotransmitter and neuromodulator, and it affects target cells by binding and activating receptors on the cell surface. As a neurotransmitter in cholinergic systems, Ach transmits information from nerve cells to other cells, such as in muscle innervations and in the autonomic nervous system. In the autonomic nervous system, acetylcholine participates in both "rest and digest" and "fight or flight" actions, which are controlled respectively by the parasympathetic nervous system and sympathetic nervous system. Importantly, Ach acts as the final transmitter in the parasympathetic nervous system, as for example in mediating the inhibitory effects of vagal nerve on the heart. As a neuromodulator, Ach plays an important role in attention, arousal, drug addiction and sleep in the central nervous system (CNS) and peripheral nervous system (PNS) (Jones, 2005). In addition, studies suggest that Ach is a critical component in modulating dopamine release in the striatum by acting on pre-synaptic nicotinic AchRs of dopaminergic neurons (Sambasivarao et al., 2013).

Acetylcholine Receptors: Muscarinic and Nicotinic

Acetylcholine functions differently in various systems, because it binds to different receptors, to regulate their corresponding pathways. There are two major classes of acetylcholine receptors, metabotropic muscarinic and ionotropic nicotinic AchRs (Albuquerque 2009). Muscarinic acetylcholine receptors (mAchRs) are G protein-coupled receptors, and their effect on target cells can be either excitatory or inhibitory depending on the subtype that is activated. mAchRs are distributed in both CNS and PNS. Nicotinic acetylcholine receptors (nAchRs) are ligand-gated ion channels; Ach or other agonist binding promotes the opening of the channel. The opening of these channels allow ions to pass through, and they have been found in both CNS, PNS and periphery. There are two main types of nAchRs, including the muscle-type and neuronal-type receptors (Papke 2008). In 1905, the English physiologist John N. Langley, first described AchRs as "receptive substance". In the following decades, more and more researchers used different approaches to study and characterize nAchRs. The first was a pharmacological approach, by using novel chemical ligands to distinguish and characterize Ach receptors. The second approach was utilizing electrophysiological techniques to study how the receptors interact with neurotransmitters. The third approach focused on the chemical composition of the receptor by using biochemical methods (Changeux, 2012). In the late 1960s, the muscle-type nAchRs were studied intensively by utilizing the *Torpedo marmorata* electrical organ, to understand the ligand-gated ion channel mechanism (Albuquerque, 2009). Later, neuronal-type nAchRs were characterized in mammalian brain (Albuquerque, 2009).

The Structure of the Nicotinic Acetylcholine Receptor

Immunochemistry studies have shown that nAchR is a heteropentamer, consisting of five subunits (two α, one β, one γ and one δ) that differ in both immunological properties and molecular weight (Lindstrom et al., 1979). Later studies suggested that in the muscle-type nAchRs, α1, β1, γ and δ subunits are expressed in the embryonic form with a ratio of 2:1:1:1. However, in the adult form, only α (α2-α10) and β (β2-β4) subunits are expressed in various combinations. The ion channel is formed between the subunits; upon agonists binding, the channel opens to allow passage of ions. The two domains of the nAchR, include the transmembrane domain and the extracellular domain, or ligand binding domain; each of the subunits share similar structures in both domains. All the subunits have long extracellular N-terminal sequences and short C-terminal sequences, and each has four transmembrane segments and an extracellular cytoplasmic loop that are believed to engage the binding of agonists (Albuquerque 2009). In each of the cytoplasmic loops of α subunit, there are a pair cysteine residues (C192 and C193) forming a disulfide bridge, near where agonists bind (Lukas et al., 1999). Despite the focus on the α-subunit as the ligand-binding site, other neighboring subunits also contribute to form the binding site and assemble the receptor. The interface between subunits are believed to the binding site for Ach (Wonnacott and Barik, 2007).

The Assembly and Locations of Nicotinic Acetylcholine Receptor Subunits

There have been ten α (α1-α10) and four β (β1-β4) subunits identified for vertebrates, and they assemble into pentamers in different combinations that dictate their

physiological functions in the nervous system and periphery (Lukas et al., 1999; Sambasivarao et al., 2013). nAchRs, are found within the cell membrane at the cell surface, and expressed in different systems, which include the PNS, CNS, and autonomic nervous system (ANS), as well as in a variety of mammalian tissues and cell types, including lymphocytes, fibroblasts, granulocytes, placenta and sensory organs. The distribution of nAchRs has been studied with pharmacological approaches, by using nAchR selective inhibitors, such as decamethonium and hexamethonium that selectively inhibit nAchRs in muscles and ANS respectively. The assembly of subunits into various types of functional nAchRs is modulated by the interaction of amino acid residues at subunit interfaces, and it is thought that the ligand binding pocket is part of the subunit interface. Besides assisting in ion channel formation, subunits that assemble into different combinations have different interaction with ligands in terms of binding, which directly affects ion channel activity (Lukas et al., 1999).

nAchRs subunits have been derived from chick, mouse, human, rat and electric ray. In human, $(\alpha1)_2\beta1\gamma\delta$ and $(\alpha1)_2\beta1\varepsilon\delta$ are naturally expressed in fetal and adult skeletal muscles respectively. Several different combinations of subunits express in the autonomic ganglia, including α3β4*(* indicates the receptor possibly contains additional subunits), α3α5β4, and α3α5β2β4. In the CNS, both $(\alpha4)_2(\beta2)_3$ and c4α5β2 are expressed. The α7* subunits express in both autonomic ganglia and the CNS, and α9* expresses in both cochlea and pituitary. Interestingly, α8 subunits are only observed in chick (Lukas et al., 1999). These receptor combinations have been characterized by expressing them in various cell lines, such as *Xenopus* oocytes, as described below.

The Functional Properties of Nicotinic Acetylcholine Receptor Subunits

It has been a challenge to determine the functional properties of individual nAchR subunits, because they can only be isolated through denaturation (Kurosaki et al., 1987). This problem was overcome by Kurisaki et al., who used the cloned subunit cDNAs to direct the formation of functional nAchRs. These cloned cDNAs have been transcribed into subunit-specific mRNAs, which can be expressed in *Xenopus* oocytes. This study suggested that the δ subunit participates in channel-gating activities, and both γ and ε subunits are involved in muscle development. It has been shown the nAchRs without either β, γ, or δ subunits have low channel activities (Kurosaki et al., 1987). Lukas et al. concluded the interfaces between α2, α3, α4 or α6 subunits and β2 or β4 subunits contain ligand binding pockets, and α5 or β3 subunits have an effect on ligand selectivity.

There are reciprocal interactions between the nicotinic acetylcholine receptors and dopaminergic neurons in the brain. First, nicotine stimulates dopaminergic neurons, especially in nigrostriatal and mesolimbic pathways, acting on various nAchR subunits that form multiple nAchR subtypes for mediating diverse behaviors. In addition, there are presynaptic nAchRs located on the striatal terminals, which promotes the activity of dopaminergic neurons to facilitate goal-directed behaviors and reinforcement that are usually missed in neurodegenerative diseases. (Azam et al., 2002; Exley and Cragg, 2008). Several studies suggest nAchR receptors containing α6 or β3 subunits regulate dopaminergic neurons. β3 subunits enhance the functional expression of α6β2β3* and α6β3β4* nAchRs in mouse (Dash et al., 2014). These receptor combinations are involved in modulating dopamine and related behaviors, changes in locomotion and other related behaviors have been observed when β3 subunit was deprived (Cui et al., 2003). α6

subunits are expressed in catecholaminergic neurons including retina, and α6 nAchRs regulate dopamine-related behaviors by modulating dopamine release in the nigrostriatal pathway (Dash et al., 2014). Depriving nAchRs that contain the α6 subunit is observed in Parkinson's disease or other neurodegenerative diseases (Sambasivarao et al., 2013).

In order to identify the nAchR subunits that express within the dopaminergic neurons of substantia nigra (SN) and ventral tegmental area (VTA), double-labeling *in situ* hybridization was performed by Azam et al., (2002). Tyrosine hydroxylase was labeled by digoxigenin-labeled riboprobe, as dopaminergic cell markers, and the ^{35}S-labeled riboprobe was used for labeling the mRNAs of nAchR subunits. They found varied expression of nAchR subunits in these regions. The expression pattern of the mRNAs of nAchR subunits was very similar in the SN and VTA, except that a lower number of dopaminergic neurons in VTA exhibited mRNA for nAchR subunit expression. Based on the results, they speculated there are different subtypes of nAchR associated with the dopaminergic neurons in both of these regions and that regulate the release of dopamine (Azam et al., 2002). β3 subunit has a very restricted expression, but is abundant in VTA and SN regions. To identify a population of nAchRs, that are β3 dependent, bind to α-conotoxin MII specifically, and modulate the release of dopamine from the striatum, Cui et al. (2003) performed both behavioral studies as well as radiolabeling *in situ* hybridization. By deleting the β3 subunit, they observed an alternation in locomotion in mice. Radioactive isotopes and α-bungarotoxin were used to label the β3 subunit in coronal slices from mice with *in situ* hybridization to visualize and quantify the intensity of mRNA signals. This showed the incorporation of β3 subunit into various striatal nAchR populations. Based on the results, they concluded that various

subtypes of nAchR containing β3 subunit and sensitive to α-conotoxin MII binding, are significant in regulating the neurotransmission of dopamine in nigrostriatal pathway (Cui et al., 2003).

Electrophysiological Studies of Ion Channel Function

In physiological studies of membrane proteins, especially ion channels, voltage clamp recordings of *Xenopus* oocytes or mammalian cells lines are indispensable to provide functional characterization of ion channel function (Dascal, 2000). In the *Xenopus* oocyte expression system, exogenous membrane proteins can be expressed individually or in combination with other isoforms, which allows one to study and compare the characteristics between wild type, mutated and chimeric proteins. There are several advantages of using the *Xenopus* oocytes expression system to study ion channels or membrane receptors. The large cell size of oocytes facilitates RNA injection and electrode penetration during electrophysiological measurements. Oocytes are isolated, washed with collagenase and kept in culture. They deteriorate in a relative slow rate, which offers a sufficient window of time (3 to 5 days) to perform electrophysiological recordings. Most of the time, healthy oocytes can survive through electrode insertion and last for hours of electrophysiological recordings (Dascal, 2000). Another advantage of using *Xenopus* oocytes to study ion channels or membrane receptors is they only express mRNA injected, because unfertilized oocytes don't express their own membrane proteins (Lodish et al., 2016). Due to this reason, the *Xenopus* oocyte expression system eliminates the possibility of responses from undesired membrane proteins during electrophysiological recordings.

The common techniques that can be performed for whole-cell or single-channel recordings are two-electrode voltage clamp (TEVC) and patch clamp, respectively. Low-resistance electrodes are often used in TEVC to study modulation and by neurotransmitters and effects of mutant or chimeric ion channels on voltage-dependence, or ion channel kinetics. Different patch clamp recording configurations can be performed in *Xenopus* oocytes depending on the research interest, including cell-attached, inside-out and outside-out configurations (Lodish et al. 2016). These configurations can be used to study single or multiple channels. Patch clamp techniques provide an insight into single-channel kinetics, as well as the effects of extracellular and intracellular reagents on channel function. Almost all aspects of ion channel kinetics and properties can be studied by combining both TEVC and patch clamp (Dascal 2000). I used two-electrode voltage clamp to investigate the effects of mutations in in the C-loop of both α3-β2 and β2-α3 interfaces for Ach binding to the nicotinic receptor.

Computational Studies

Computational modeling and simulation are powerful tools that allow researchers to test hypotheses, gain insights and understandings of questions, interpret and refine functional studies, integrate knowledge and information, and inspire new ideas and approaches. As computational approaches have become more advanced, they have been used by researchers as a complement to functional studies. Along with functional studies, computational approaches help researchers to explain questions at a more rigorous level to provide a deeper understanding of mechanisms and structures of complex systems. The general purposes of computational modeling and simulation are to create the models of

systems based on the known structural information and mimic the mechanisms of these systems under given conditions. Predictions from computational studies can be compared to the results from functional and theoretical studies to draw conclusions.

While computational modeling is an extremely useful tool, it requires the understanding of mathematical, algorithmic and conceptual knowledge needed to create models, as well as the values and limitations of models. It is very critical to choose which software to use to create model depending on the interest of study, because different software use different algorithm and mathematical equations that are better at one or some areas than the others. A major advantage of using computational modeling is that it is less time-consuming to produce a significant amount of comparative data. Homology models can be used to elucidate whether or not particular mechanisms are sufficient enough to cause certain results or occurrences. Sometimes, when the results from functional studies and computational studies don't agree with each other, such differences may inspire new approaches to address the question of interest (Brodland 2015).

Several examples of employing a computational approach to address questions relevant to my thesis work are described below. Mallipeddi et al. (2013) used homology modeling to generate the structure of mammalian nAchR from the *Torpedo californica* α2βδγ nAchR, and molecular dynamics to simulate the interactions between residues and ligand for different receptor conformations. Molecular dynamics simulations revealed that in the α-subunit, there are the H-bond interactions between Y190 and Y93 in agonist-binding sites or with K145 adjacent to the binding site. There are side chain interactions between K145 and D200, and a main chain interaction between K145 and Y93. Other residues including W149, Y198 in α-subunit, L108, L118 and Y116 in γ-subunit, L111,

T119 and L121 in δ-subunit appear to be associated with stabilizing ligands in ligand-binding sites. A computational study from Schapira et al. (2002) using the homology model that was built based on *Lymnaea stagnails* Ach binding protein suggests cation-π interaction between the quaternary ammonium group of acetylcholine and tryptophan in the binding pocket. They aligned the sequence of *Lymnaea* AchBP and mammalian nAchR for α3, 4 7 and β2, 4 in building the homology model. The computational results also demonstrate the Van der Waals interaction between Ach and Trp182, Tyr230, and Cys225-225 in the α-4 subunit, and Trp82, Leu146 and Phe114 in the β2 subunit. They also suggest that water molecules in the binding pocket form hydrogen bonds with Ach that further stabilize the Ach in the binding pocket. Their computational results showed there is no interaction between the ester group of Ach and residues in the binding pocket, a result contradicted by the previous photoaffinity labeling experiment (Schapira et al., 2002). It is thought that the Trp149 and Tyr 93 are important in establishing the cation-π interaction, as well as the cation-binding domain in the agonist binding site. Tyr190 and Tyr198 are involved in interacting with the ester moiety of Ach (Hu et al., 2010). Since there are many aromatic residues in the agonist binding pocket are involved in ligand binding, Beene et al. (2004) took a step forward to investigate how tyrosine may effect ligand binding and channel gating mechanisms using AutoDock, and unnatural amino acid substitutions. Their computational results showed the hydrogen bonds formed by Tyr143 and Tyr 153 are important in stabilizing the receptor in ligand-bound state, which may also be critical in changing the receptor conformation towards gating. Additionally, their computational results suggest that Tyr 143 and Tyr153 are in proximity in the closed state even they are located on separate β sheets, but their combined movements may

provide a significant torsional force as showed during a docking simulation (Beene et al., 2004). Open and closed state homology models were built based on the template structures of *Aplysia californica* nicotinic acetylcholine binding protein and *Torpedo marmorata* nicotinic acetylocholine receptor respectively by Sambasivarao et al., (2013). Their simulation results suggested that various aromatic residues, such tyrosine and tryptophan, play critical roles in Ach binding in the binding pocket of both α3 and β2 subunits. For α-conotoxin MII binding, negative charged residues are important in the binding pocket of both subunits.

Early investigations of the ligand-binding sites of nAchRs involved functional studies. As the role of computational studies have become more and more important as a tool of investigation, more researchers have combined computational studies and functional studies to explore the structure-function relationships (Beene et al, 2004). I used TEV to provide functional data on Ach binding in the C-loop of α3β2 nAchR, and homology modeling with MOE simulations to investigate the effect of mutations in the C-loop of both α3-β2 and β2-α3 interfaces for Ach and α-conotoxin MII binding. This work is presented as a step towards understanding the role of these and similar nAcRs in the dopaminergic pathways in the brain and to help provide new approaches to pharmacological intervention in dopamine disorders.

MATERIALS AND METHODS

The care and use of animals (*Xenaopus* laevis) of this study followed protocol 730, which was approved by the Institutional Animal Care and Use Committee (IACUC) at Idaho State University.

Chemicals and Solutions

All chemicals for electrophysiology were obtained from Sigma Chemical or Thermo Fisher Scientific. Agonist (acetylcholine, in the form of acetylcholine chloride) was made as 0.1M stock solution in bath solution before each experiment, and kept on ice. The oocyte bath solution consisted of 96 mM NaCl, 2 mM KCl, 1 mM $MgCl_2$, 1.8 mM $CaCl_2$, 5 mM HEPES, 1 μM atropine (antagonist of muscarinic Ach receptors), at pH 7.4±0.05. The oocyte culture medium contained 96 mM NaCl, 2 mM KCl, 1 mM $MgCl_2$, 1.8 mM $CaCl_2$, 5 mM HEPES, 2.5 mM sodium pyruvate, and 100 mg/L gentamicin sulfate with 4% heat-inactivated horse serum, at pH 7.4±0.05.

Expressing nAchR α3β2 Subunits in *Xenopus* Oocytes: mRNA Injection

The rat neuronal nAchR subunits α3 and β2 were contained in plasmid vectors pSP64 and pSP65, respectively. Plasmid vector pSP64 was linearized by *EcoRI*, and pSP65 was linearized by *HindIII*. After they had been linearized, the restriction digests were used as templates, using SP6 RNA polymerase (mMESSAGE mMACHINE Kit, Thermo Fisher Scientific) to make messenger RNA (mRNA). Equivalent mass of mRNA for each subunit was injected into *Xenopus* oocytes at stage 5 or 6, using a total volume of 50 nL mRNA. After the oocytes had been injected, they were incubated in culture

medium with gentle shaking at 17.5°C for at least 3 days before recordings using voltage clamp electrophysiology (Figure 1).

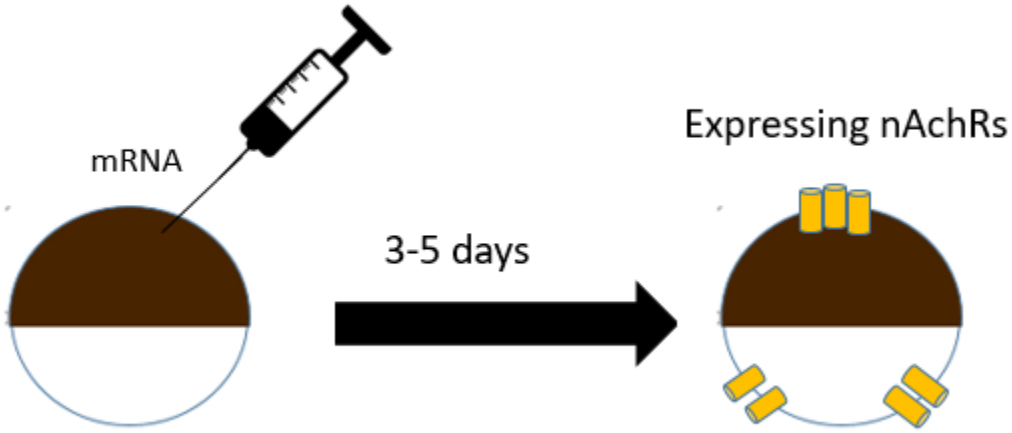

Figure 1. *Xenopus* oocyte expressed nAchRs on the cell surface after 3-5 days of mRNA injection.

Electrophysiology (Two-electrode voltage clamp)

The voltage recording and current passing electrodes had resistances of 4 to 7 MΩ, after they were filled with 3M KCl solution. An oocyte was placed in the recording chamber (Warner Instruments RC-1Z), and perfused with the oocyte bath solution at a rate of ~1.5ml/min continuously throughout the entire experiment. An upright microscope (Meiji EMZ) was used to visualize the oocyte, and Narashige YOU-1 manipulators were used to impale the oocyte with each electrode. Membrane potential was recorded and clamped with Warner OC-725C amplifier and data were acquired with PatchMaster 2.35 (HEKA), using an ITC-18 digitizing interface, with software run on

MacIntosh G5 computers, OSX 10.4. All recordings were done at room temperature of 20 to 21°C. The voltage clamp protocol, started at -70mV for 1 second, and then at -80mV for 16 seconds before return to -70mV. The acetylcholine was applied 3 second into the -80mV segment, with application of 1 ml in 1 second.

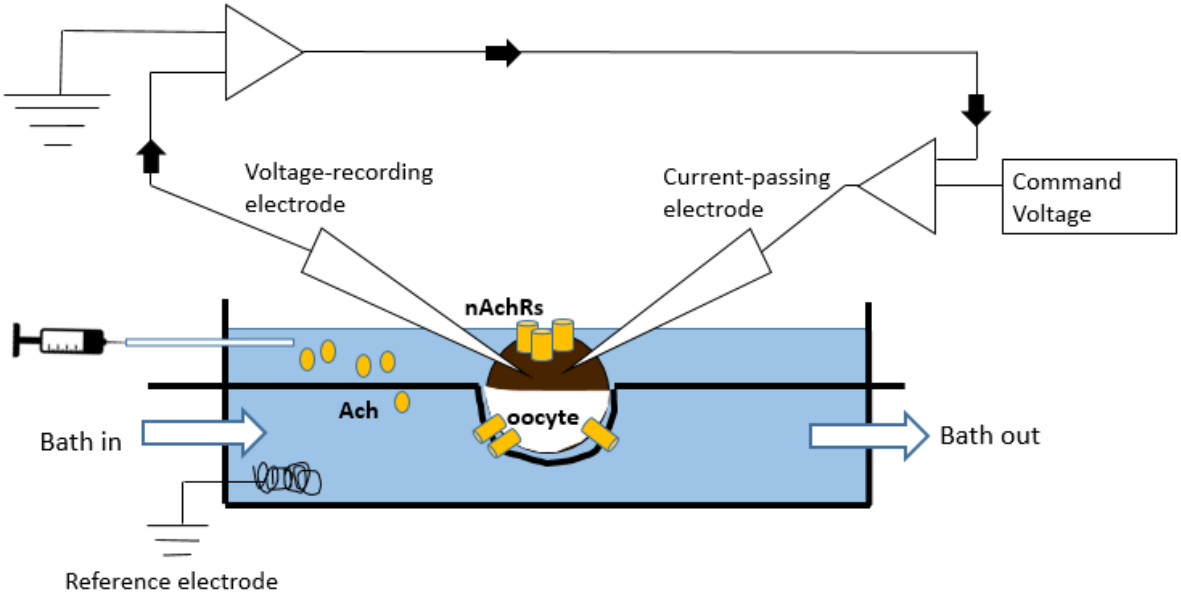

Figure 2. Basic electrical set-up for the two-electrode voltage clamp (TEVC) with the *Xenopus* oocyte inside the recording chamber.

Between trials, oocytes were held at -70 mV. The amplitudes of the inward currents were measured by subtracting the mean amplitudes of leak current at -80mV prior to application of Ach, from the maximal amplitudes in response to Ach. Average membrane potentials for oocytes before voltage clamp were approximately -18 mV. Application of the bath solution was used as control prior to each application of Ach. The concentrations of Ach that was used in experiments ranged from 1 nM to 30 mM for all mutations, and each was prepared from the 0.1M stock solution. Ach was applied in 1 ml aliquots in approximately 2 seconds with a syringe attached to the recording chamber. To

make sure there was no Ach left in the plastic tube or the recording chamber, bath solution was applied manually between each application of Ach. The time interval between two acetylcholine applications were 6-8 minutes depending on previous concentration: a longer time interval was required with higher concentrations of Ach to insure recovery from receptor desensitization.

Data Analyses

The overall goal of exploring different analytical methods was to find a better way to fit the data from functional studies. By comparing these analyses use different equations and parameters to produce a fit for the data, the analysis that produced the best fit for the data was selected. The table below lists parameters that used by each type of analyses.

Table 1. The following illustrates the parameters that used in each type of analyses. Also refer to the equations for each type of analyses in the latter section.

Type of Analysis	Parameters
Scatchard	• B-the amount of bound ligand • F-the amount of free or unbound ligand • Bmax-the total concentration of receptor • Kd-dissociation constant
Eadie-Hofstee	• Bmax • B

	• F • Vmax- maximal velocity at saturating substrate concentration • V-velocity of the reaction • S-substrate concentration • Kd • Km-the substrate concentration when the reaction rate is half of Vmax
Lineweaver-Burke	• V • Vmax • Km • V • S
Hill	• Vmax (max in the equation) • V_0 – the initial velocity of the reaction (base in the equation) • EC_{50} ($x_{1/2}$ in the equation) or Km

Scatchard and Eadie-Hofstee Analyses

Scatchard analyses are often used for transform the data from saturation curves that are produced by partially selective ligands. When there are receptor subtypes, Scatchard analysis yields a curvilinear relationship rather than a linear plot. When

applying Eadie-Hofstee method to analyze the data of using selective competitors, it often generates a displacement curve. Eadie-Hofstee analysis produces a curvilinear plot in the presence of receptor subtypes. Both Scatchard and Eadie-Hofstee methods are very similar in a way that their axes are simply reversed. Scatchard method plots B/F on y-axis, and B on x-axis. Eadie-Hofstee has its axes reversed (B on y-axis, B/F on x-axis). The x and y intercepts are also reversed for Scatchard and Eadie-Hofstee plots, and it's easier to estimate the degree of accuracy of y intercept than x intercept with linear regression analysis. A limitation for both Scatchard and Eadie-Hofstee methods may occur when adenylate cyclase is involved in the process of activating or inhibiting the receptors. The results could be misrepresented as in presence of receptor subtypes in curvilinear plots. The advantage of applying Scatchard and Eadie-Hofstee analyses is they both have the property of homogeneity of variance, which eliminates the weighting in the linear regression analysis and so the SD of amount bound is proportional to the amount bound (Molinoff et al., 1981; Attie and Raines, 1995).

There are additional problems associated with Scatchard and Eadie-Hofstee analyses, such as B/F, or both B and B/F, cannot be estimated precisely. Errors can be present in B measurement or in both B and B/F axes. The larger the error present in the data, the larger is the underestimate of both Bmax and Kd.

These two methods involve the B or F (amount bound/free ligand) see below in their equations, which often applied in studies that use radioactive ligand or any radiolabeling that allows the measurements of B or F. The reason that these two methods cannot be applied to analyze the functional data in this study is the two variables that being measured were the response to Ach and the concentration of Ach, which cannot be

plotted with either equation. There were no values of B, F, Bmax or Kd generated from the functional experiments (see Table 1 above) Thus, both methods were not used.

Scatchard Equation:

$$\frac{B}{F} = \frac{Bmax}{Kd} - \frac{(\frac{1}{Kd})}{B}$$

Eadie-Hofstee Equations:

V=Vmax-Km*(V/S)

B=Bmax-Kd*(B/F)

Lineweaver-Burke Method

Another statistical analysis that is appropriate to use when the data are log transformed and was able to fit with a linear relationship. The Lineweaver-Burke method is also known as the double-reciprocal equation that plots the reciprocal of V (rate of reaction) against the reciprocal of S (concentration of substrate) (Zivin and Waud, 1982). This method assumes equal spread of data points along the line (homogeneity of variance). Since it's the double-reciprocal equation, the low substrate concentration and rate of reaction are indicated that results in any small mistakes in measuring these low values to be magnified. This method was used to analyze the functional data in this study,

where S was the concentration of Ach and V was the maximal of response to Ach. Unfortunately, this method did not provide a good fit for the data.

Lineweaver-Burke Equation:

$$\frac{1}{V} = \frac{1}{Vmax} + \frac{(Km/Vmax)}{S}$$

The following graphs show the experimental data (Ach binding to wild type receptor) fitted with the Lineweaver-Burke equation (Figure 3) versus the Hill equation (Figure 4), and clearly the Hill equation generated a better fit for the data than using the Lineweaver-Burke equation.

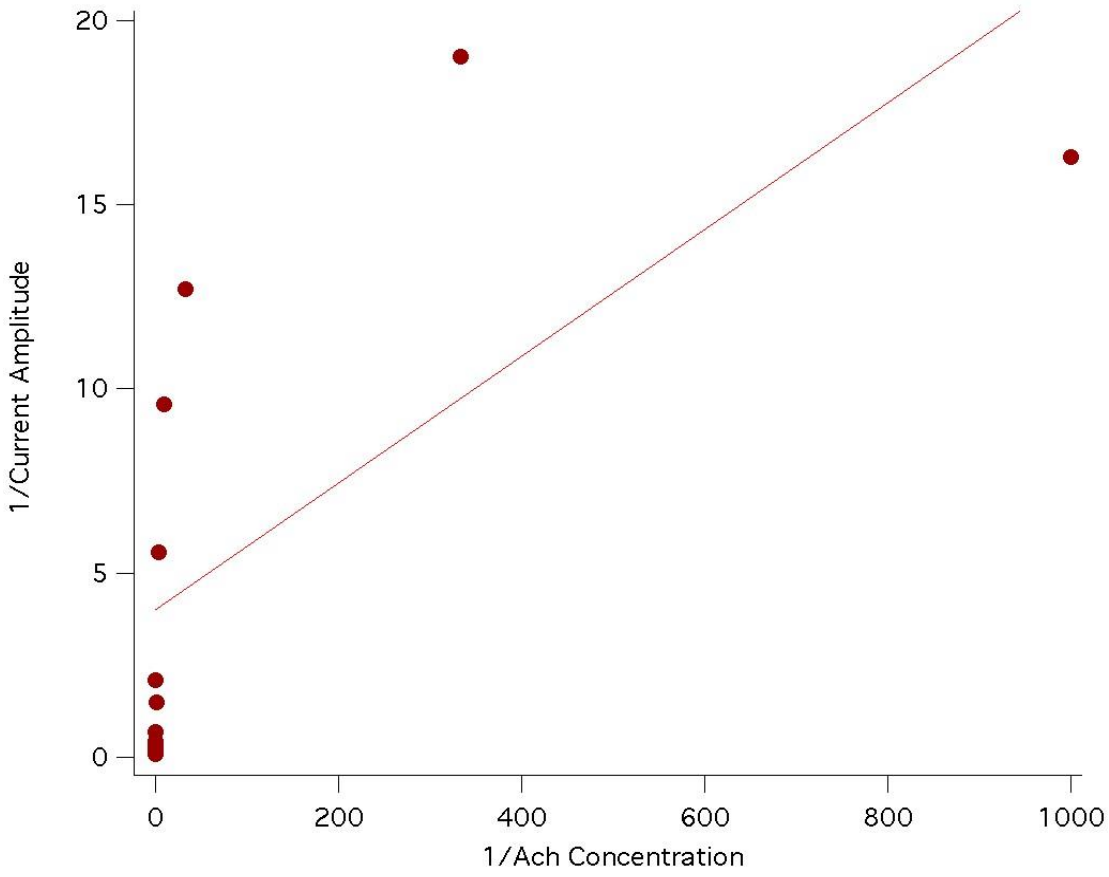

Figure 3. A linear fit for the data that was produced by using the Lineweaver-Burke equation.

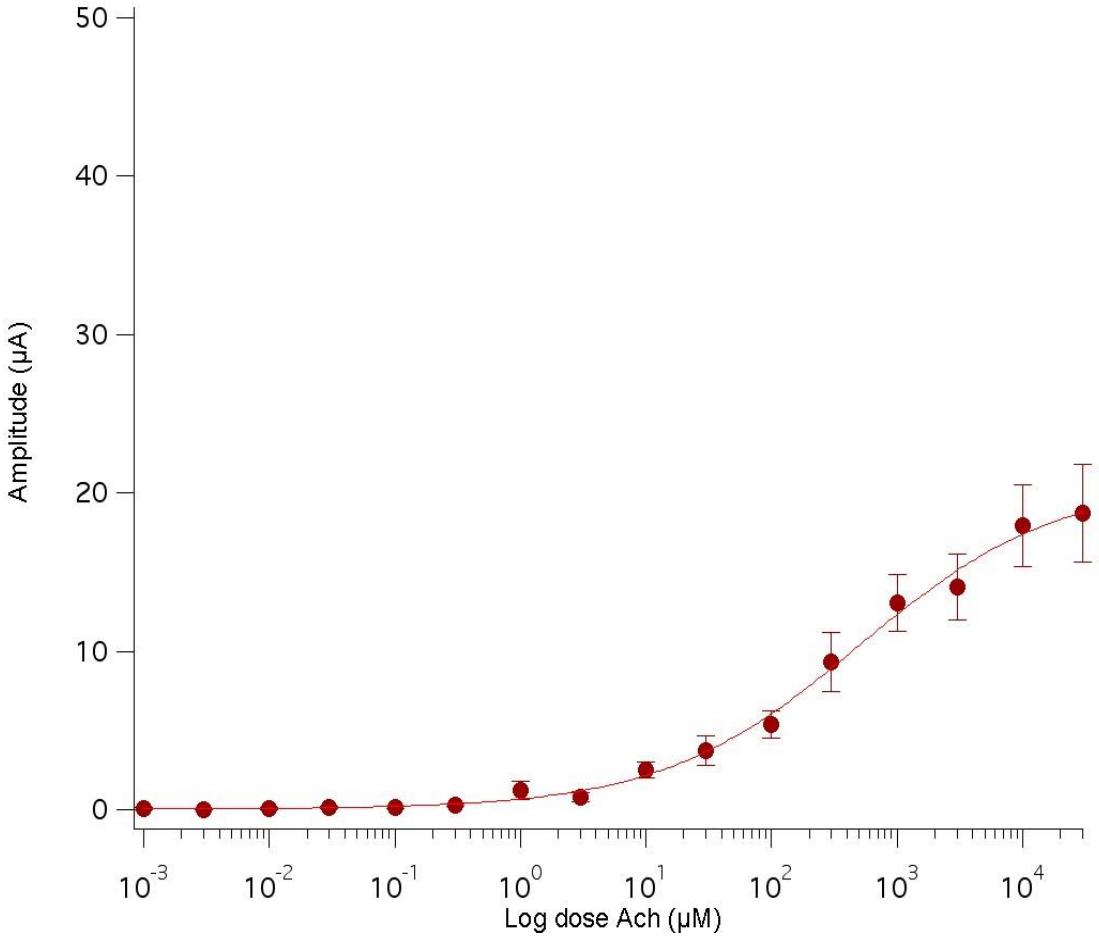

Figure 4. A dose response curve for the data that was produced by using the Hill equation.

Hill Equation

The Hill equation is often used to measure the affinity of ligand for its receptor (or other interactions) by estimating the dose for half-maximal response (excitatory concentration) as the EC_{50}, and the asymptote for the maximal response. This equation (Hill, 1910) was first used to describe the binding of oxygen and hemoglobin. Under extreme positive cooperativity between the binding of the first and subsequent ligands, the Hill coefficient can accurately estimate the number of binding sites. However, this coefficient is not a reliable indicator because extreme positive cooperativity cannot always be assumed, in which case the Hill coefficient can only minimally estimate the number of binding sites involved. When there is significant positive cooperativity present in both sequential and independent bindings, the Hill coefficient can accurately estimate the number of ligand binding sites. Multimeric receptors that often have binding sites located on different subunits, such as ligand-gated ion channels, often fall into the category of independent binding, therefore Hill equation often can be effectively used from dose-response curves based on the given ligand concentrations and corresponding response or bound/total ligands. Changes in cooperativity often affect the $K_{0.5}$ (or represented as EC_{50} in this study) and Hill coefficient, as the cooperativity becomes more negative the Hill coefficient decreases to close to 1 if the nAchR binding is independent not cooperative (Weiss 1997).

From my functional data, the Hill equation was the method that best fit the data from two electrode voltage clamp experiments of variable dose Ach applied versus inward current observed. I excluded data sets (recording sessions) for which the maximal response was less than 2 μA, and considered these oocytes to be poorly expressing

receptors at that time. Then, the averaged data as a function of Ach concentration was fit with the Hill equation to generate a table that consists of chi-square, minimal and maximal responses to Ach, rise rate of the curve and EC_{50} (excitatory concentration that produce half of the maximal response). Chi-square is an indicator that measures how well the function fits the data, and a small chi-square value indicates a good fitting between the function and the data.

The Hill Equation:

$$y = Base + [(max - base) / 1 + (x_{1/2} / x)^{rate}]$$

The statistical methods that I applied to analyze the computational and functional data were one-way ANOVA and post-hoc Tukey's test (with R), which compare the mean of wild type nAchR and mutant nAchR to determine whether or not they were significantly different.

Homology Model

The sequences of rat neuronal α3 and β2 subunits of the nAchR were aligned with the template sequence (open C-loop, PDB ID: 2BR8, *Ac*-AChBP) in Seaview with the Clustal aligning method. The alignment results for α3 and β2 subunits were then prepared separately into PIR format that was readable by Modeller 9.13. After all the Modeller input files were prepared, the executable file (PY file) was run to generate a homology model for one subunit (α3 or β2) at a time. For creating mutated subunits, the native

residues (C192, C193 in α3 subunits and D192, D193 in β2 subunits) were replaced with alanine in the sequences from Modeller input files. After creating the models of α3 and β2 subunits in Modeller, each of them was superimposed onto a selected chain in the template structure (PDB ID: 2BR8, *Ac*-AChBP) in Chimera by using the MatchMaker function. In order to create an interface between each pair of α3 and β2 subunits, the chains these two subunits superimposed onto were next to each other. With the exception of the interface between β2 and β2 subunits, the two β2 subunits were superimposed onto the neighboring chains. The structure along with the position coordinates of each subunit was saved as a PDB file. The final step of creating PDB files for interfaces was concatenating each pair of neighboring subunits together.

The following flowchart shows step by step how homology models (interfaces) were created by various software using template and target sequences.

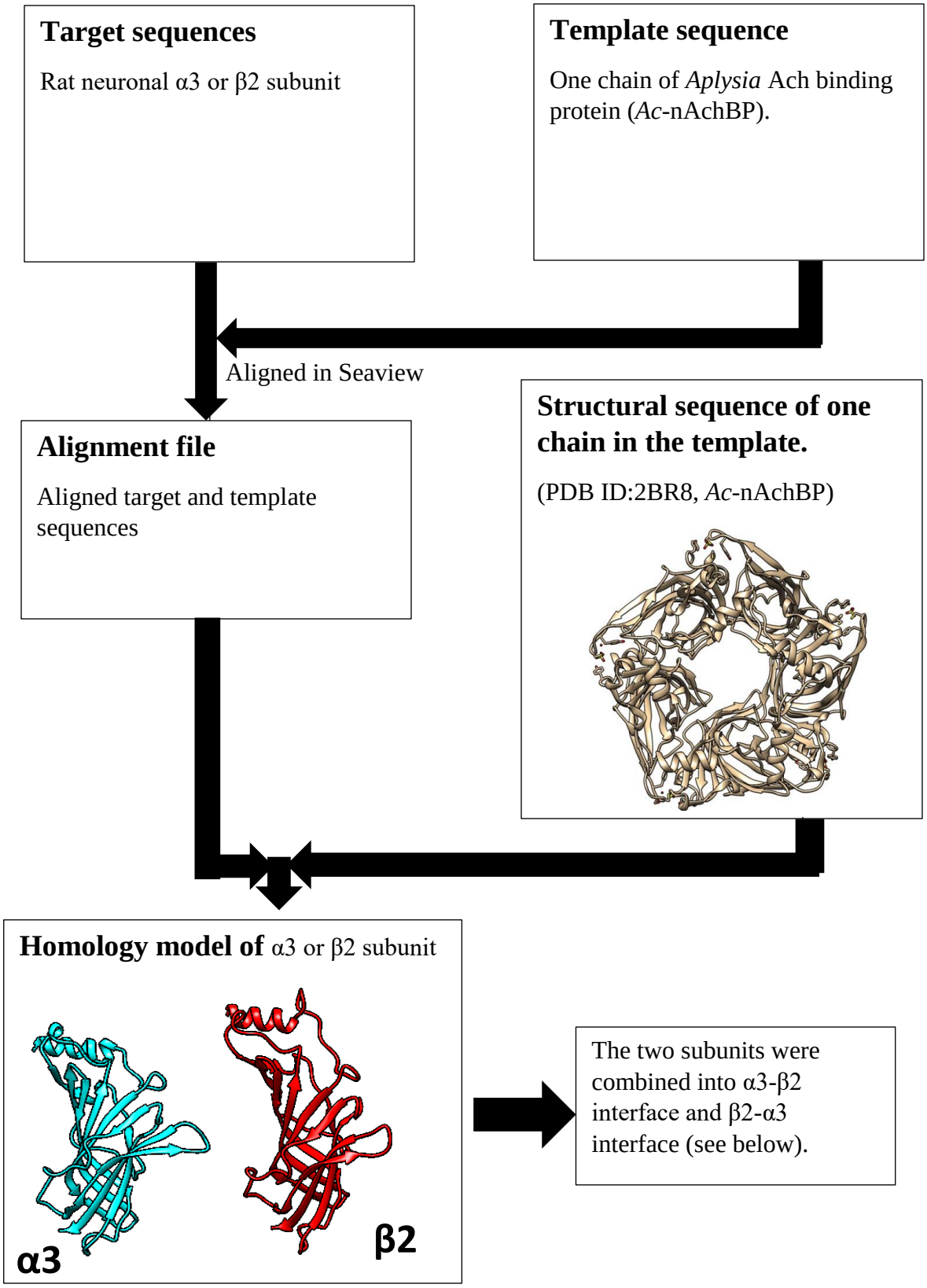

Figure 5. A flowchart that shows how the homology models were created.

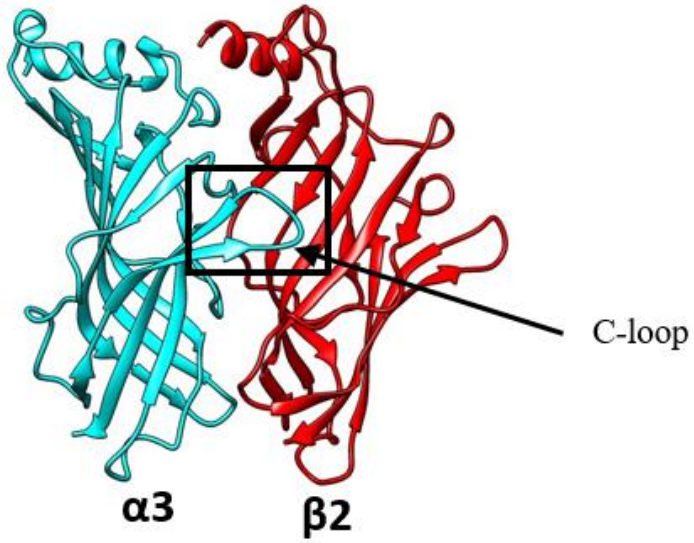

Figure 6. α3-β2 interface. The α3 subunit (cyan chain) is the primary chain that contains the C-loop, whereas the β2 subunit (red chain) is the complementary chain. Image by Chimera.

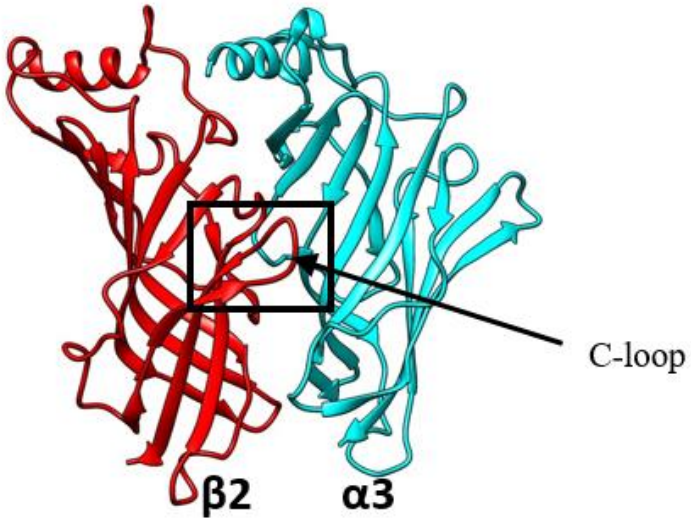

Figure 7. β2-α3 interface. The β2 subunit (red chain) is the primary chain that contains the C-loop, whereas the α3 subunit (cyan chain) is the complementary chain. Image by Chimera.

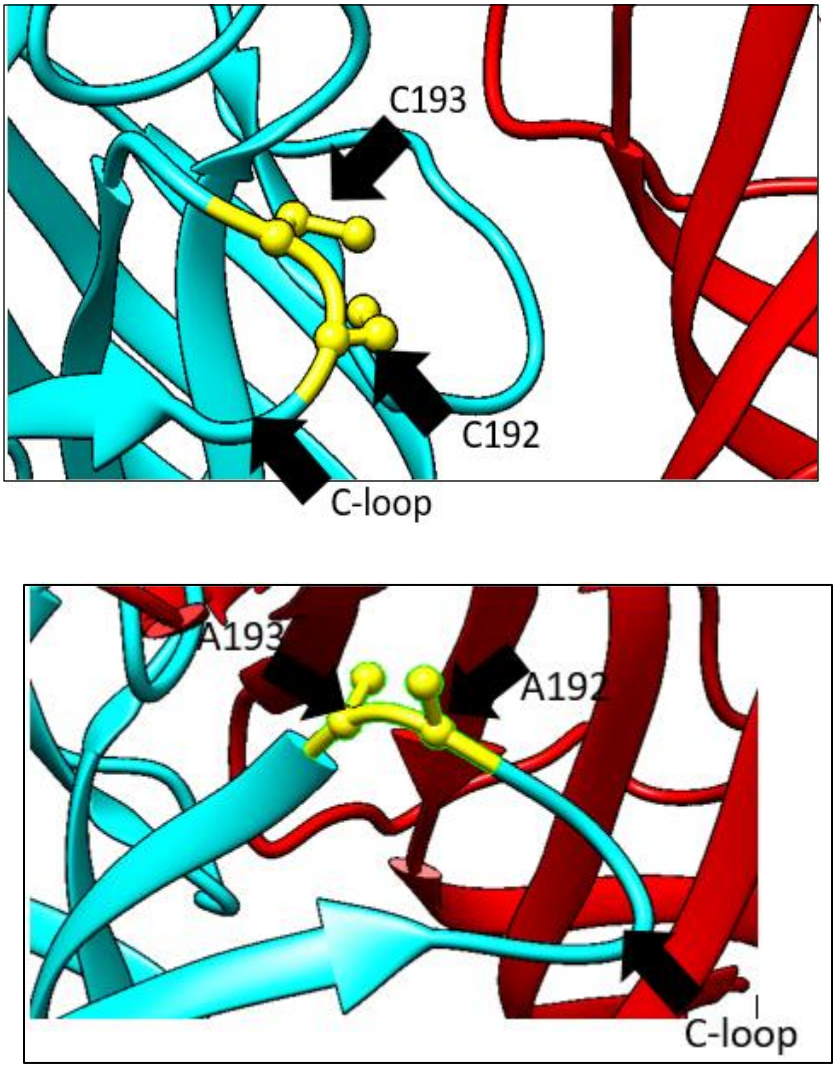

Figure 8. The Ach binding pocket of α3-β2 interface, cysteine (C192 and C193) (top picture) and alanine (A192 and A193) (bottom picture) are on the C-loop of the α3 subunit. The residues of interest are shown in yellow.

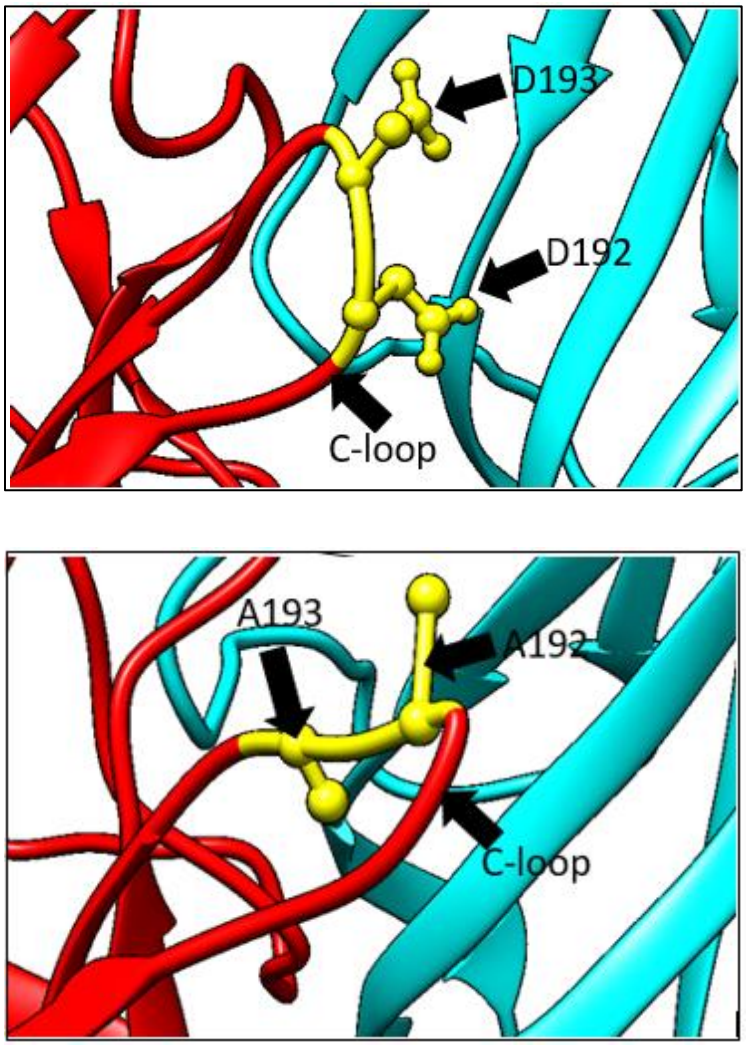

Figure 9. The Ach binding pocket of β2-α3 interface, aspartate (D192 and D193) (top picture), alanine (A192 and A193) (bottom picture) are on the C-loop of the β2 subunit. The residues of interest are shown in yellow.

MOE (molecular operating environment) Docking

Binding Wild Type Receptor with α-Conotoxin MII

The .pdb file for an interface (α3-β2 or β2-α3) was opened in MOE as the receptor, and underwent protonation for all atoms at 70 °F (room temperature), pH 7.4 and 0.1 M salt concentration. After protonation was complete, the sequence editor was used to select residues D192, D193 and D198 in the β2 subunit as binding sites for β2-α3 interface (D170, D171 on the β2 subunit and E194, E195 on the α3 subunit were selected as binding sites for α3-β2 interface, D115 on the complementary β2 subunit) and performed energy minimization. The .pdb file of α-conotoxin MII was selected as ligand. Before docking, both binding sites and ligand were selected. In the docking setting, induced fit was selected as docking protocol, the α3-β2 interface .pdb was selected as the receptor along with the above-mentioned selected residues. Ach as ligand was the selected atom, the placement was triangle matcher and refinement was by forcefield. The first scoring system was London dG, and the second scoring system was GBVI/ WSA dG. The option of removing duplicates was checked and 50 poses were retained. After setting up all parameters, docking was performed.

In order to compare the effect of each residue, or each set of residues that contribute to α-conotoxin MII binding in each interface, the residues described previously were individually, or along with other residue(s) tethered as binding site(s) to α-conotoxin MII. For α3-β2 Interface, D170, D171 on the β2 subunit and E194, E195 on the α3 subunit were tethered separately. For the β2-α3 interface, D192, D193 were tethered separately from D198.

To get a further insight into how C-loop residues may interact with α-conotoxin MII, they were mutated into alanine with protein builder function in MODELLER and tethered either individually or in a combination with other residues as described above for both interfaces.

Docking Mutated Receptor with α-Conotoxin MII

Mutated subunits were created by Modeller. In the mutated α3 subunit, the cysteines at position 192 and 193 were replaced with alanines. Aspartates in the same position in β2 subunit were also mutated to alanines. In order to validate the binding of α-conotoxin MII to homology models that were created, D170, D171 on the β2 subunit and E194, E195 on the α3 subunit were selected together and separately for α-conotoxin MII binding in α3-β2 Interface. For β2-α3 interface, A192, A193 were selected together with D198 and separately from D198 for α-conotoxin MII binding. In addition to mutations at position 192 and 193 in α3 or β2 subunits, the previous binding sites were all mutated to alanine with protein builder function in Modeller. The combination of mutated binding residues were all selected for each interface for α-conotoxin MII binding.

Table 2. The binding pockets and their corresponding selected binding sites for α-conotoxin MII. Residues that are in each cell were selected as binding sites for individual experiment. Note: (-) means the residues were on the complementary subunit and (+) indicates the residues were on the primary subunit that contained the C-loop.

Binding pocket	Selected binding sites
α3-β2 (or α3C192A/C193A-β2)	(-)D170, D171 (+)E194, E195 (or alanine at the same positions)
β2-α3 (or β2D192A/D193A-α3)	(+)D192, D193, D198 (or alanine at the same positions)

Docking Wild Type and Mutated Receptors with Ach

Previous studies have shown a group of residues, mostly aromatic, located behind the C-loop are responsible for the nAchR's binding specificity for Ach (Czajkowski and Karlin, 1994; Sambasivarao et al., 2013). When binding Ach against nAchR, many residues selected as binding sites in MOE were aromatic (e.g. tyrosine, tryptophan, phenylalanine). The procedures for Ach docking in MOE were similar to α-conotoxin MII docking. The first step was importing the receptor (α3-β2 or β2-α3 interface), which was protonated for all atoms at 70 °F (room temperature), pH 7.4 and 0.1 M salt concentration. Followed by energy minimization for wild type receptor, any mutations created by protein builder in MOE were performed prior to energy minimization. Before docking, the interface was selected as receptor, and the binding sites were Y93, W149, Y190, Y197 for the α3-β2 interface or Y95, W151, P191, Y196 for the β2-α3 interface. Ach was imported and selected as the "selected atom", and placement was triangle

matcher and refinement was by forcefield. The first scoring system was London dG, and the second scoring system was GBVI/ WSA dG. The option of removing duplicates was checked with retained 50 poses. Ach was binding against wild type receptor, receptor with mutations at position 192, 193 or both for the two types of interface. In the α3-β2 interface, mutations C192A, C193A and C192AC193A were created. In the β2-α3 interface, D192AD193A and D192CD193C were created. Each mutation was created by protein builder in MOE and docked by Ach, which conducted as a separate MOE experiment.

Table 3. The binding pockets and their corresponding selected binding sites for Ach. Residues that are in each cell were selected as binding sites for individual experiment.

Binding pocket	Selected binding sites
α3-β2 (or α3C192A/C193A-β2)	Y93, W149, Y190, Y197 (on α3 subunit)
β2-α3 (or β2D192A/D193A-α3)	Y95, W151, P191, Y196 (on β2 subunit)

RESULTS

Functional Study of Effects of Mutations in nAchR C-loop

In order to explore the specific residues in C-loop of nAchR control the access of Ach to its binding pocket, two-electrode voltage clamp recordings were used to measure inward sodium current amplitudes of response to Ach. The mean of amplitude of response to Ach for each concentration was calculated for each mutation as shown in Table 4, and these values were used to construct dose response curve to calculate the maximal response and half maximal response (EC_{50}) using the Hill equation. The dose response curve of each mutation was compared to wild type α3β2 nAchR as shown in Figure 11-13, and one-way ANOVA was used to test whether the EC_{50} between the wild type nAchR and each mutation was significantly different.

Comparisons of the dose response curves for double alanine substitutions in the α subunit (C192A/C193A) and β2 subunit (D192A/D193A) to wild type α3β2 nAchR showed a trend that alanine substitution in the α subunit C-loop increased the amplitude of response to Ach, and shifted the EC_{50} to the right, while alanine substitution in the β2 subunit C-loop decreased the response to Ach and produced a left shift of the $EC_{50.}$ I also tested the construct in which alanine substitution in each subunit was inserted (C192A/C193A/D192A/D193A). Since the dose response curves were obtained from experiments in which only a portion of the Ach concentration range was tested for any given oocyte, mean values from the Hill equation were not obtained. Instead, I compared the mean amplitude in response to a given concentration of Ach from the combined data set (Table 4).

Chi-square is the statistic that indicates how well the data fit to the Hill equation; a lesser chi-square value implies better fitting of the data to the Hill equation. By comparing all the chi-square values in Table 1 and appendix Table 1A, both quadruple mutations (C192A/C193A/D192A/D193A and C192A/C193A/D192C/D193C) had relative higher chi-square values than wild type α3β2 nAchR, single, or double mutations. Their relatively poor fit to the Hill equation may be due to their relative small sample sizes.

The Hill equation was used to determine parameters of maximal amplitude of response to Ach, and the concentration of Ach that elicited half-maximal response (EC_{50}). Most of the mutations studied did not affect the maximal response compared to wild type. However, the double mutations C192A/C193A increased the maximal response, and D192A/D193A decreased the maximal response. Another critical value from fitting the data to the Hill equation was the $EC_{50,}$ the excitatory concentration that generates half of the maximal response. C192A/C193A/D192A/D193A produced the lowest EC_{50} compared to wild type α3β2 nAchR (Table 1), and the quadruple mutation C192A/C193A/D192C/D193C produced the highest EC_{50} (Appendix, Table 1A). The other mutations tested had lower EC_{50} than wild type (with the exception of C192AC193A, which produced a higher EC_{50} than wild type).

By observing the pattern of the dose-response curve for wild type and mutations, the dose-response curve for most of these constructs did not show a plateau of response at high concentrations of Ach applied. Therefore, their maximal responses as calculated based on the highest point of the dose-response curves may not accurate, since plateaus were estimated by the Hill equation. Since EC_{50} for these mutations are also calculated

based on the estimated maximal responses, these values must be interpreted with caution. The variance for C192AC193AD192AD193A and C192AC193AD192CD193C mutations are relative large compared to the rest, which may contribute to their larger chi square values.

Table 4. Results from two-electrode voltage clamp study comparing wild type and mutant α3β2 nAchR. Maximal response and half maximal response (EC_{50}) parameters were obtained from fits to the data using the Hill equation.

Mutations	Chi square	Average maximal response (μA)	EC_{50} (μM)	Average response to 1mM Ach (μA)	Sample size (n)
α3b2 (WT)	3.02	20.74	496.39	13.07±1.83	37
C192A/C193A	7.06	24.28	587.29	14.43±1.54	61
D192A/D193A	9.32	14.07	291.69	11.85±2.06	19
C192A/C193A/ D192A/D193A	16.86	17.42	19.83	16.77±3.04	17

The average response for 1 mM Ach of wild type α3β2 nAchR, double mutations C192A/C193A, D192A/D193A and the quadruple mutation C192A/C193A/D192A/D193A nAchR were plotted in a histogram for comparison.

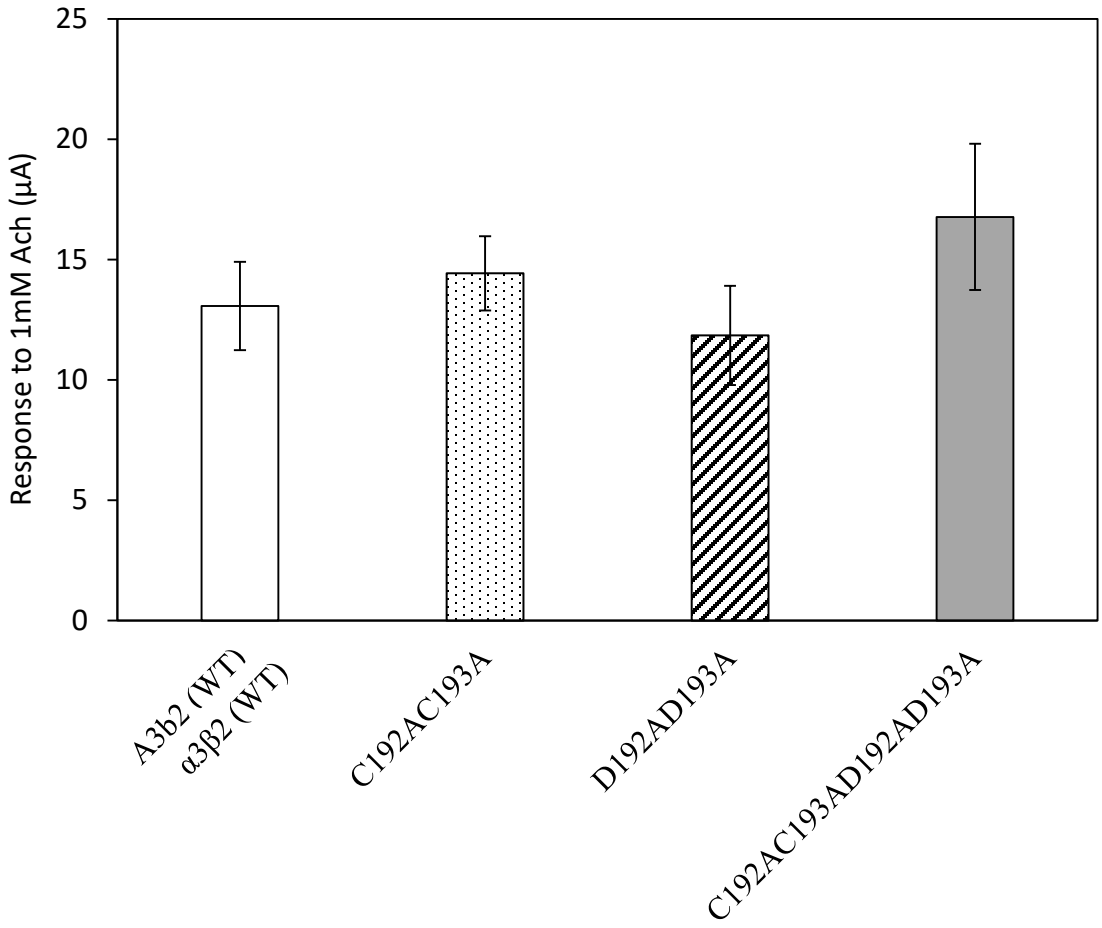

Figure 10. The average responses to Ach in amplitude (μA) ± SEM for wild type, D192A/D193A, C192A/C193A and C192A/C193A/D193A/D193A.

The amplitude of response to 1 mM Ach of wild type nAchRs and mutants nAchRs, as well as their dose-response curves are shown below:

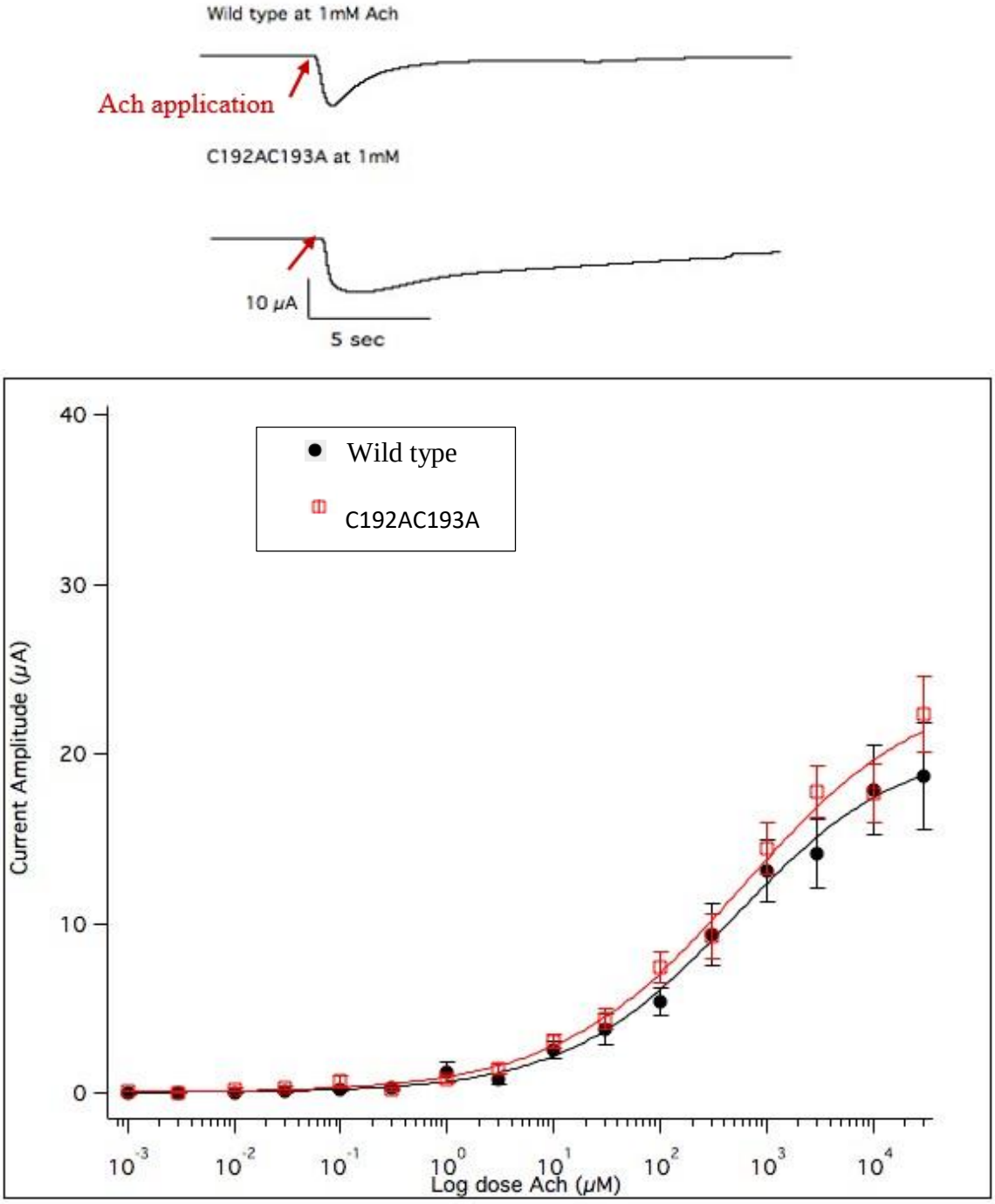

Figure 11. The dose response curves of wild type and mutant C192A/C193A. Lines represent the fit to each data set using the Hill equation. Insets on top of the dose response curve show the response to 1 mM Ach, and red arrows indicate where Ach was applied.

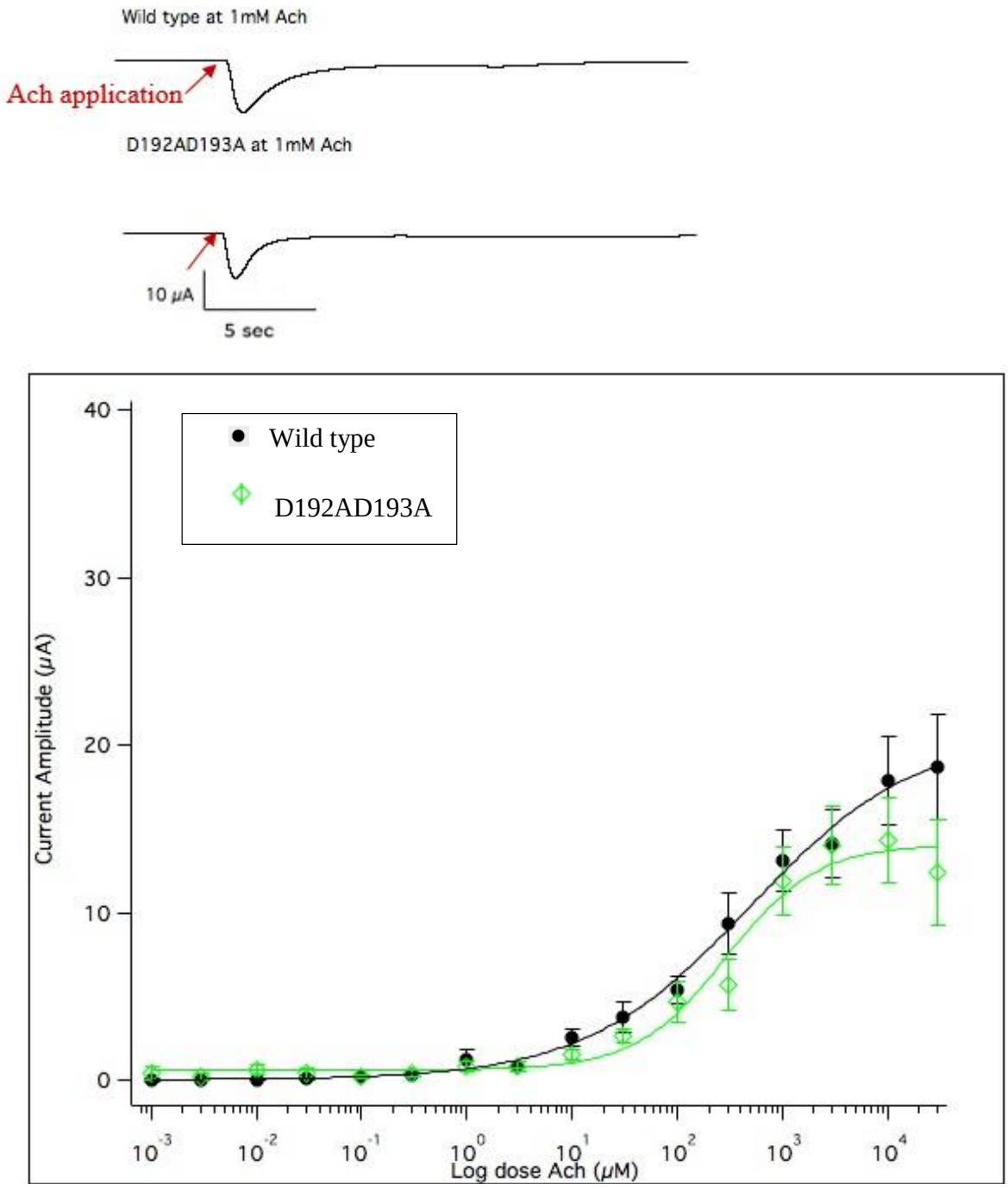

Figure 12. The dose response curves of wild type and mutant D192A/D193A. Lines represent the fit to each data set using the Hill equation. Insets on top of the dose response curve show the response to 1 mM Ach, and red arrows indicate where Ach was applied.

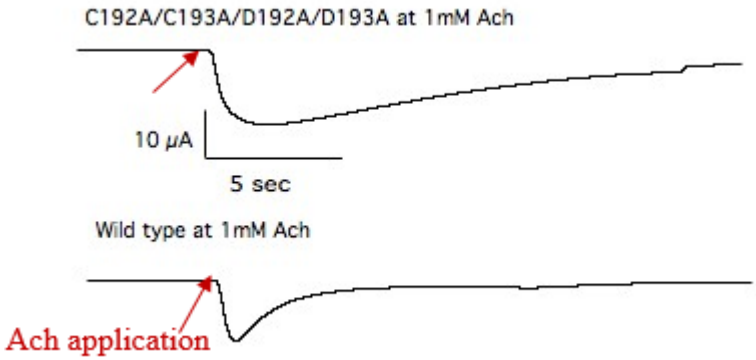

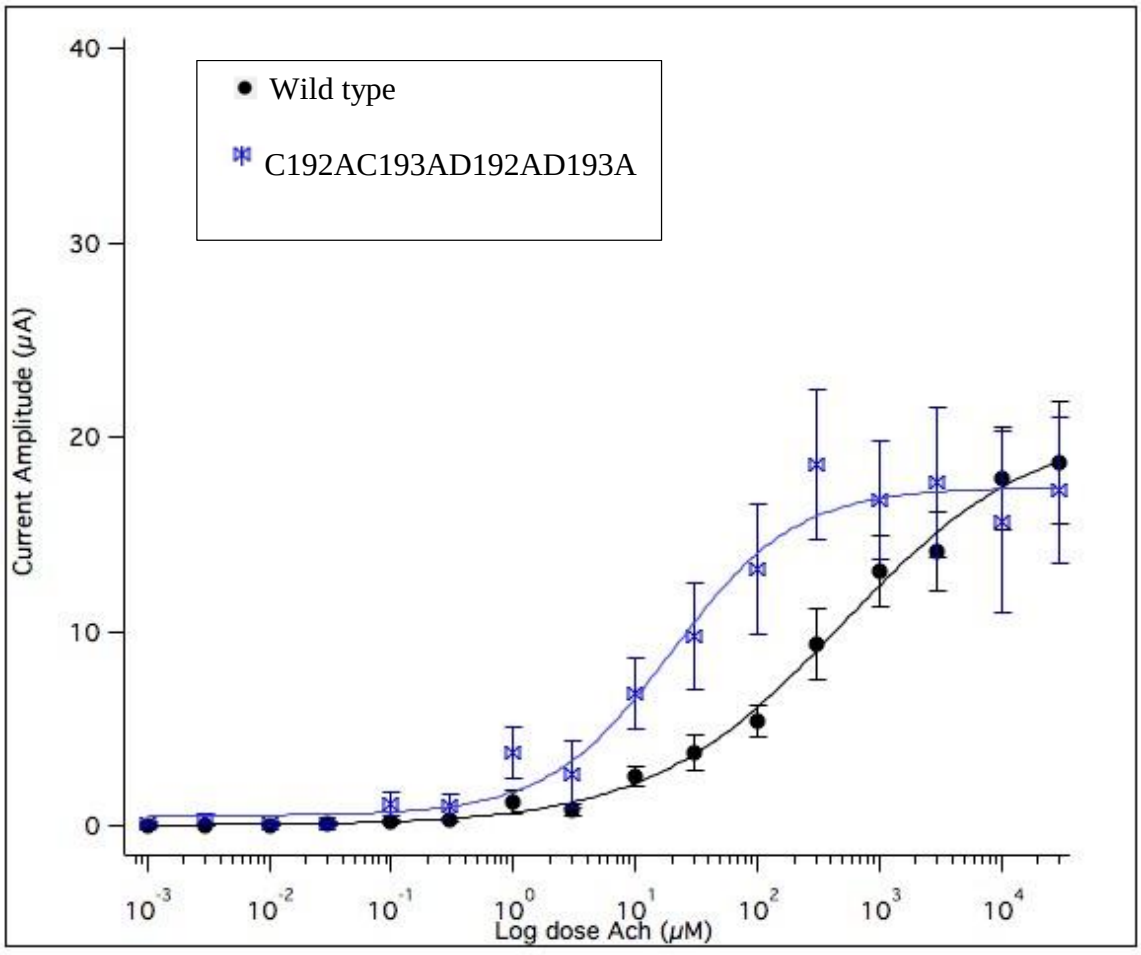

Figure 13. The dose response curves of wild type and mutant C192A/C193A/D192A/D193A. Lines represent the fit to each data set using the Hill

equation. Insets on top of the dose response curve show the response to 1 mM Ach, and red arrows indicate where Ach was applied.

Homology Modeling and MOE Simulations

The goal of homology modeling is to provide a visualization of the structure of the mammalian nAchR based on protein sequence alignment with a similar AchR for which structural information is available from the Protein Data Bank. Homology models, wild type and mutants, were created by computational modeling and further used in MOE simulation. New hypotheses, predictions and interpretations can be developed based on the structure of the model, which including the proximity of residues and the characteristics of neighboring residues. MOE simulation puts the homology nAchR models into the environments with given pressure, temperature, pH, and other conditions to generate energy outputs when a ligand (Ach) is allowed to interact with the binding region. By comparing energy outputs between MOE simulations using wild type and mutated nAchR models, the effects of mutated residue(s) can be revealed. MOE simulations on Ach binding were used as a complement to functional studies to assist in testing the hypotheses that residues C192/C193 in the α3 subunit, and D192/D193 in the β2 subunit, regulate the binding of Ach. The results of MOE simulations provide valuable information that can be used to refine the functional experiments and develop future directions.

I also used MOE simulations to compare α-conotoxin MII binding to wild type and mutatant nAchRs, to test the hypothesis that these residues (C192A/C193A and D192A/D193A) are part of the binding site for conotoxin.

The following figures show the C-loop residues of interest in homology model α3-β2 (Figure 14) and β2-α3 (Figure 15) interfaces. The top and bottom diagrams in each figure are compared to show the difference in terms of structures of the wild type C-loop residues versus after they have been mutated. Both figures below illustrate where C-loop is located on the interfaces.

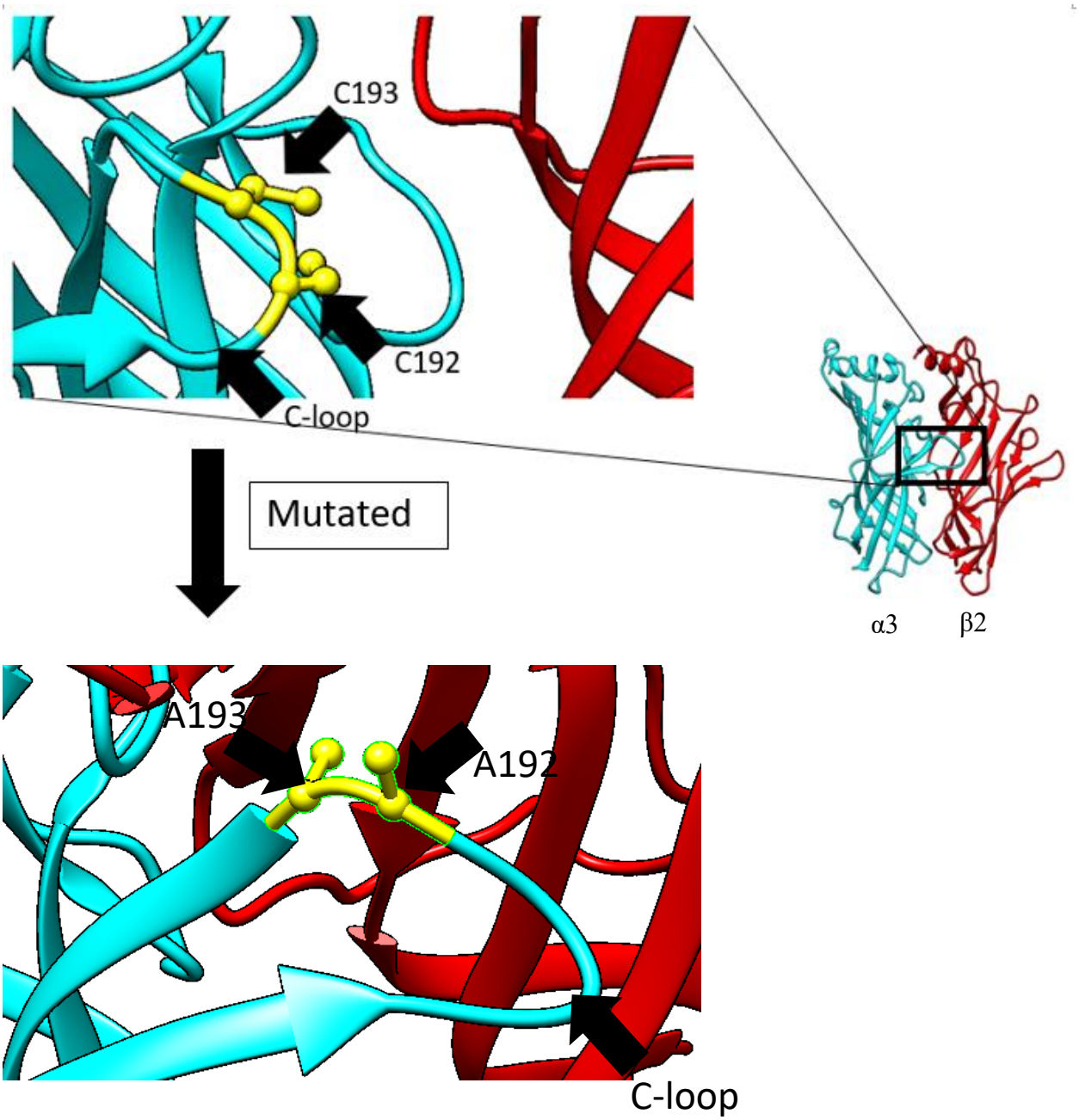

Figure 14. α3-β2 interface. The α3 subunit (cyan chain) is the primary chain that contains the C-loop, whereas the β2 subunit (red chain) is the complementary chain. Image by Chimera. The residues at position 192 and 193 are shown in yellow, for the native cysteine (top) and for alanine substitutions (bottom).

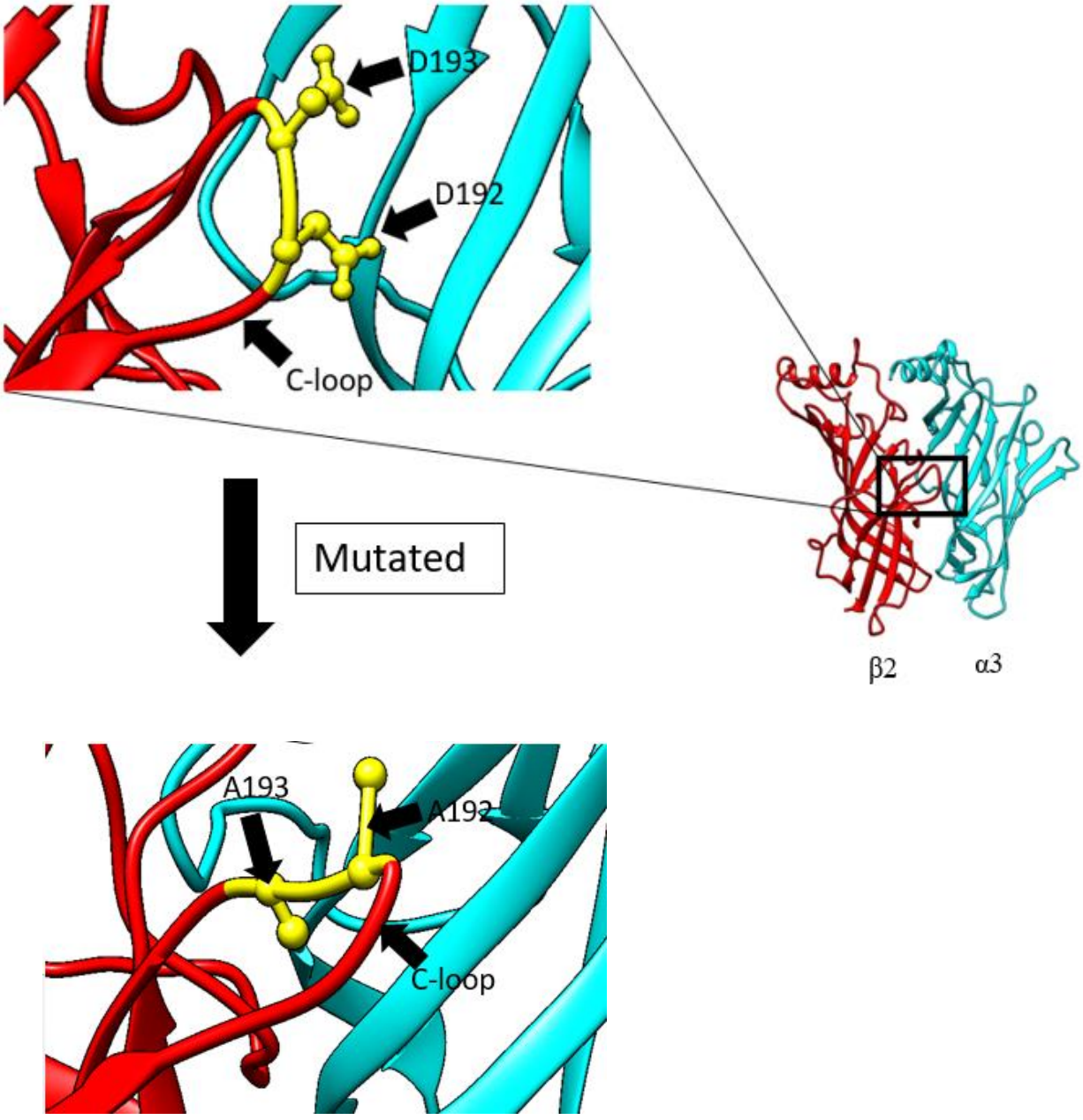

Figure 15. β2-α3 interface. The β2 subunit (red chain) is the primary chain that contains the C-loop, whereas the α3 subunit (cyan chain) is the complementary chain. Image by Chimera. The residues at position 192 and 193 are shown in yellow, for the native aspartates (top) and for alanine substitutions (bottom).

Computational Results of Ach Binding

To validate the use of MOE for Ach binding, the docking results of wild type receptors binding Ach were compared between the same interfaces, among different interfaces (Table 2) and to the docking results from Sambasivarao et al. (2013).

Two α3-β2 interfaces and two β2-α3 interfaces were constructed as with the native nAchR orientation, and docked to Ach to produce free binding energies (exothermicities). The average free binding energies for the interfaces are very similar (Table 2). α3-β2 interfaces produced a higher average binding energy than β2-α3 interfaces. The standard deviation for all interfaces are similar, and the number of retained poses for all of them is close to 10 except for one of the β2-α3 interfaces. One-way ANOVA and post-hoc Tukey's test revealed the average free binding energy between the same interfaces were not significantly different. The values of average binding energy from Table 2 were compared to the corresponding values from Sambasivarao et al (2013) (α3-β2 interface open state generated a binding energy of -5.0±0.1 kcal/mol for Ach binding, and -5.1±0.2 kcal/mol for β2-α3 interface), and they were very similar.

Table 5. The results produced by docking Ach to various receptor binding pockets using MOE. Both α3-β2 interfaces had same selected binding sites, and two β2-α3 interfaces also had the same selected binding sites.

Binding Pocket	Average free binding energy (kcal/mol)	Standard deviation of free binding energy	Number of total retained poses
α3-β2 interface (B chain-C chain)	-3.88	0.65	8
α3-β2 interface (E chain-A chain)	-4.04	0.27	10
β2-α3 interface (A chain-B chain)	-4.14	0.46	9
β2-α3 interface (D chain-E chain)	-4.19	0.48	5
β2-β2 interface (C chain-D chain)	-3.83	0.52	13

In order to understand the effects of mutations on Ach binding, the docking results of wild type receptors binding Ach (α3-β2 interface and β2-α3 interface) were compared to the results from their mutated receptors (Table 6 and Table 7, respectively). Each docking of a mutated interface with Ach was conducted as a single experiment, and Ach was tethered to the same binding sites in wild type receptors and their mutated receptors. However, both one-way ANOVA (overall p-value > 0.05) and post-hoc Tukey's tests suggested there are no significant difference between means of free binding energy of those mutations compared to the wild types.

In Table 6, the docking result from wild type α3-β2 interface is compared to the docking results from mutated (C192A/C193A) α3-β2 interface. The one-way ANOVA (overall p-value > 0.05) and post-hoc Tukey's test suggested there are no significant difference between mean of free binding energy of the mutant compared to wild type.

Table 6. The results produced by docking Ach to mutated α3-β2 interface.

Binding Pocket	Average free binding energy (kcal/mol)	Standard deviation of free binding energy	Number of total retained poses
WT	-4.04	0.27	10
C192AC193A	-4.00	0.31	6

The energy for binding Ach to wild type and mutant (C192A/C193A) nAchRs are compared in a histogram (see below).

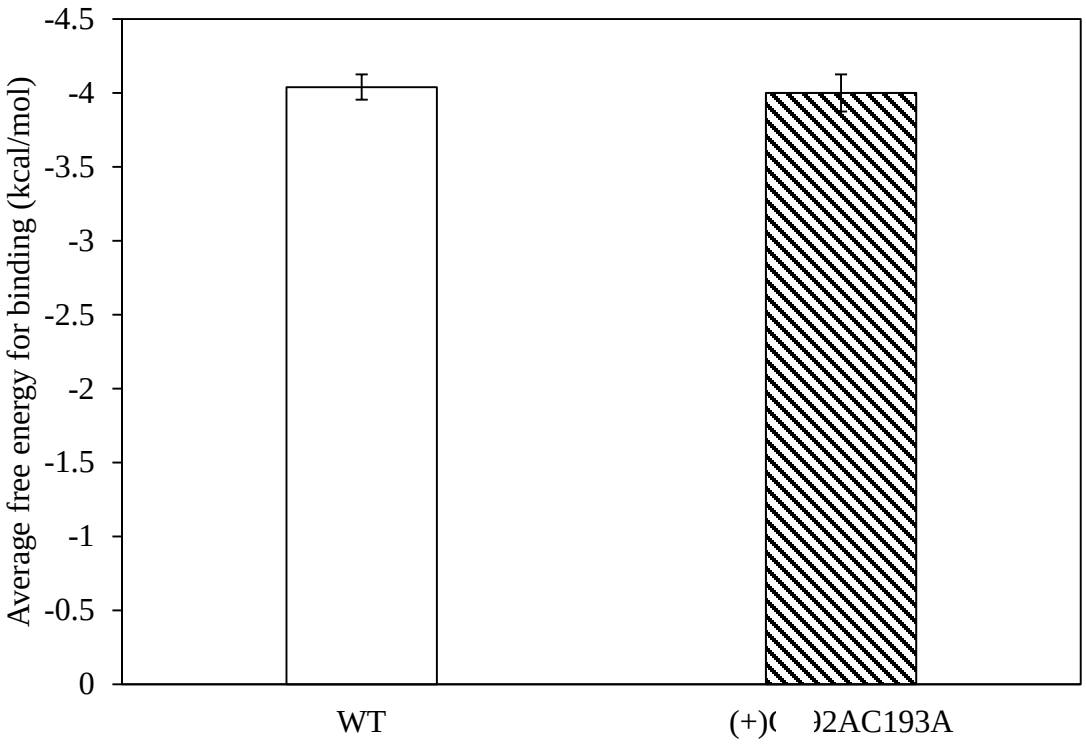

Figure 16. The average binding energy (kcal/mol) ± SEM of docking Ach to α3-β2 binding pockets that containing no mutations (WT) and mutant C192AC193A.

MOE provides the visualization of interactions between Ach and the wild type α3-β2 binding pocket residues. These residues include predominantly tryptophan (57, 149), and tyrosine (93, 190, and 197), and aspartate (152, 171, 199), plus isoleucine 119, arginine 81 and serine 148 in the binding pocket of α3-β2 interface.

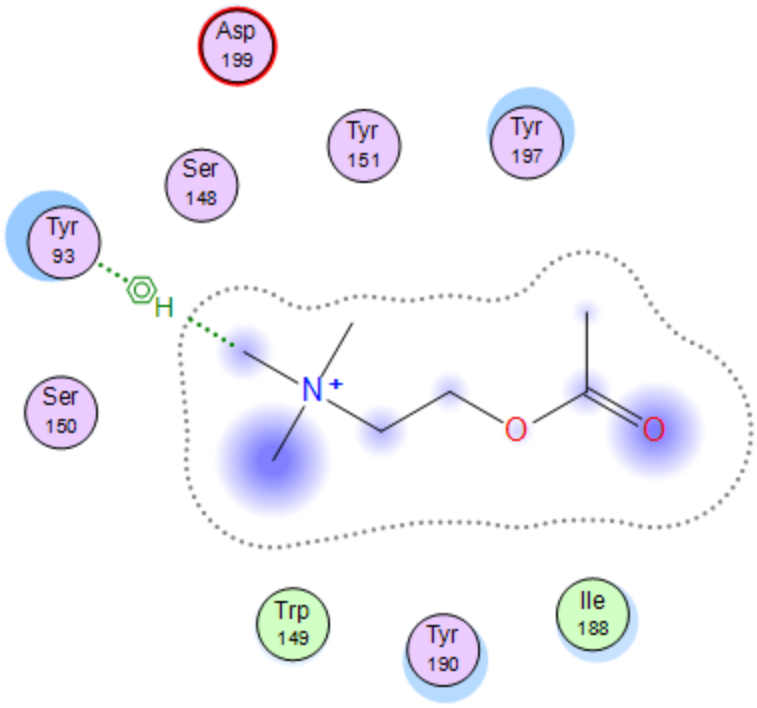

Figure 17. A 2-D diagram illustrates how Ach molecule interacts with various residues in the binding pocket of α3-β2 interface.

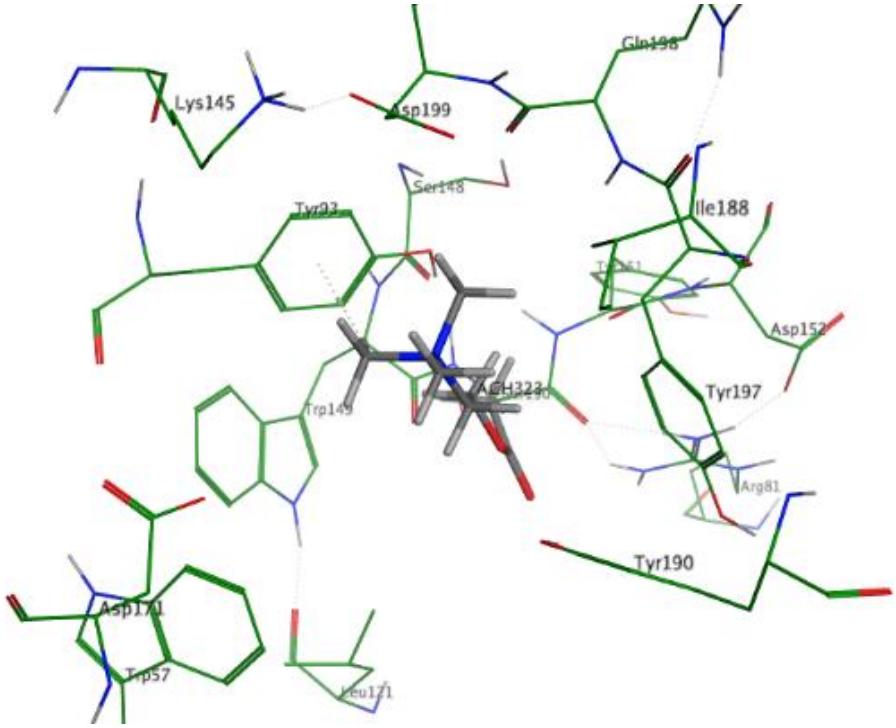

Figure 18. Ach (thick grey structure) in the binding pocket of α3-β2 interface, the ester group of Ach is pointing into the plane. The residues (Y93, S148, W149, S150, Y151, I188, Y190, Y197, D199) that interact with Ach in the binding pocket are labeled. Image by MOE.

In Table 4, the docking result from wild type β2-α3 interface is compared to the docking results from mutated (D192A/D193A) β2-α3 interface. The one-way ANOVA (overall p-value > 0.05) and post-hoc Tukey's test suggested there are no significant difference between mean of free binding energy of the mutant compared to the wild type.

Table 7. The results produced by docking Ach to mutated β2-α3 interface

Binding Pocket	Average free binding energy (kcal/mol)	Standard deviation of free binding energy	Number of total retained poses
WT	-4.14	0.46	9
D192AD193A	-3.82	1.03	7

The energy for binding α-conotoxin MII to wild type and mutant (D192A/D193A) nAchRs are compared in a histogram (see below).

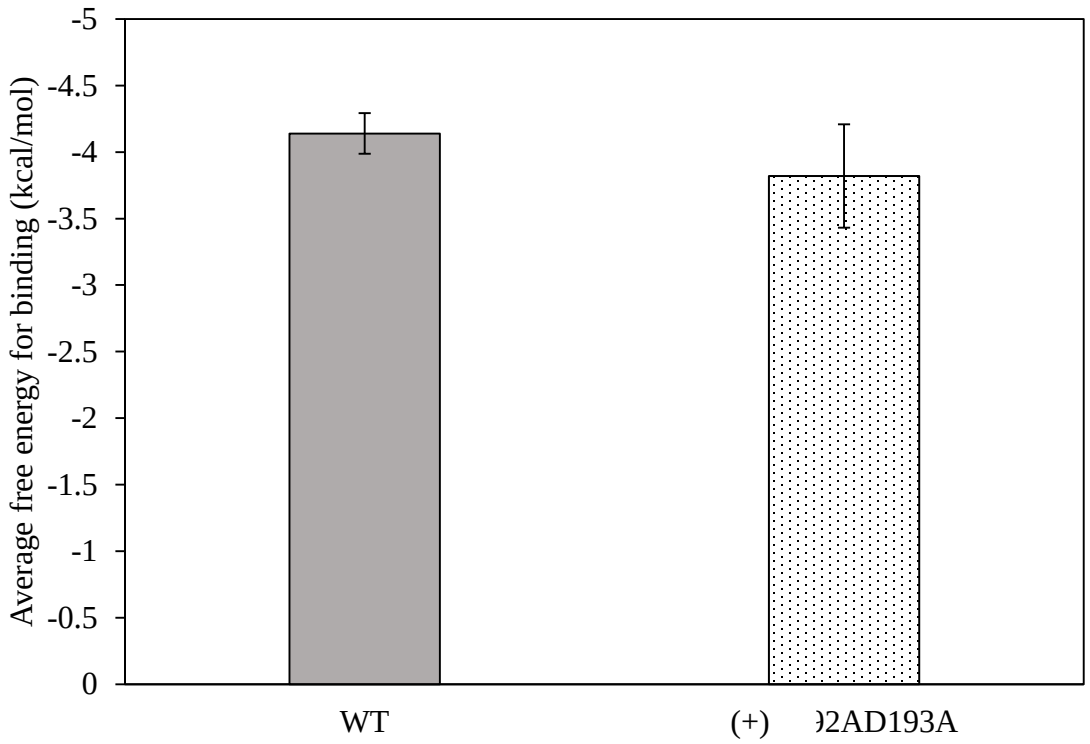

Figure 19. The average binding energy (kcal/mol) ± SEM of docking Ach to β2-α3 binding pockets that containing no mutations (WT), and mutant D192AD193A.

MOE provides the visualization of interactions between Ach and the wild type α3-β2 binding pocket residues, which are mostly aromatic. In the binding pocket of β2-α3 interface, tryptophan (55, 151, 171), tyrosine (93, 196), aspartate (99, 103, 104, 152), isoleucine 123, and serine 38.

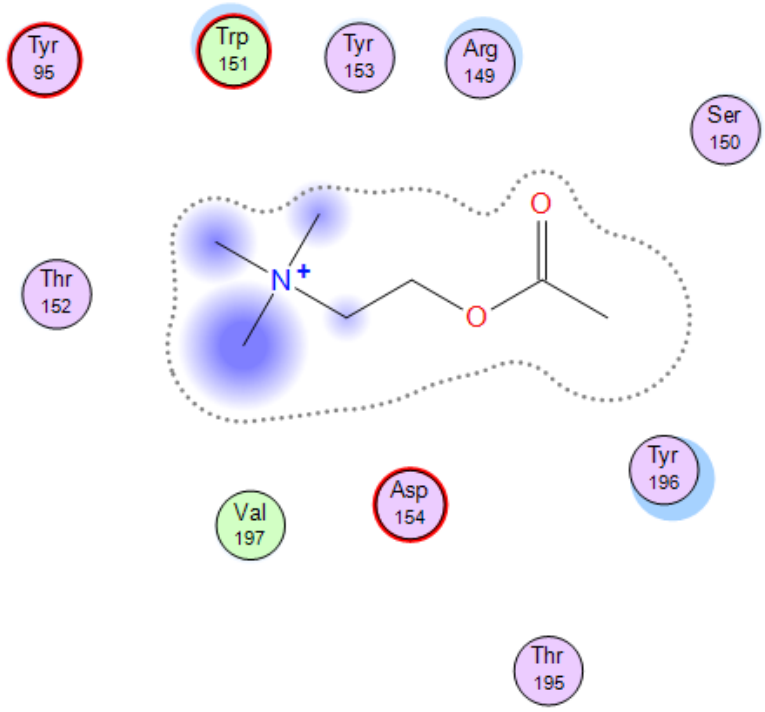

Figure 20. A 2-D diagram illustrates how Ach molecule interacts with various residues in the binding pocket of β2-α3 interface. Image by MOE.

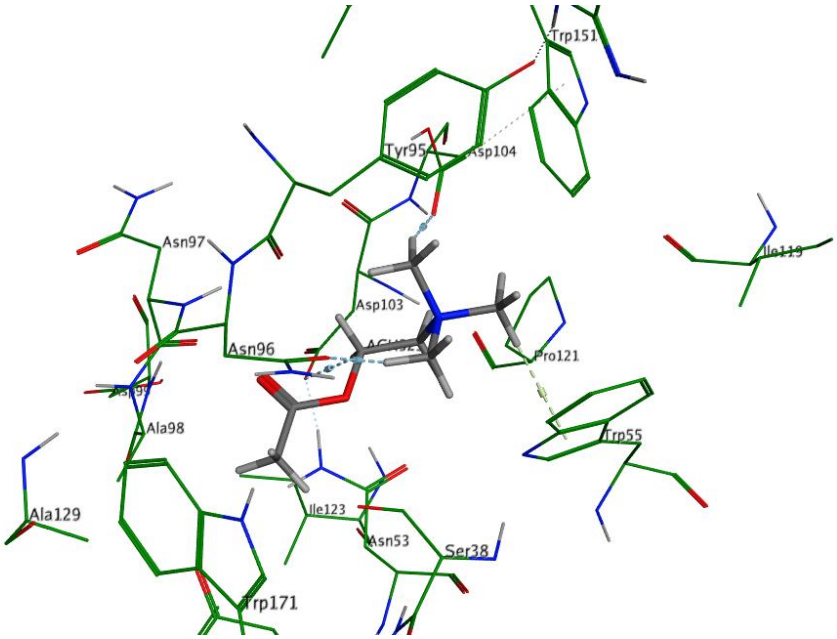

Figure 21. Ach (thick grey structure) in the binding pocket of β2- α3 interface, the ammonium ion group of the Ach interacts with the labeled residues (Y95, R149, S150, W151, T152, Y153, D154, T195, Y196, V197) in the binding pocket. Image by MOE.

Computational Results of α-Conotoxin MII Binding

To validate the use of MOE for α-conotoxin MII binding, the docking results of wild type receptors (α3-β2 interface and β2-α3 interface) to α-conotoxin MII are compared between the same interfaces, among different interfaces (Table 8), and to the results from Sambasivarao et al. (2013). One-way ANOVA showed no significant difference in the average free binding energy between the same interfaces with docking to α-conotoxin MII (p-value > 0.05) in Table 5.

Table 8. The results produced by docking α-conotoxin MII to various binding pockets. Both α3-β2 interfaces had same selected binding sites, and two β2-α3 interfaces also had the same selected binding sites.

Wild type receptor	Average free binding energy (kcal/mol)	Standard deviation of free binding energy	Number of total retained poses
α3-β2 interface (B chain-C chain)	-4.89	0.54	46
α3-β2 interface (E chain-A chain)	-4.22	0.85	37
β2-α3 interface (A chain-B chain)	-3.53	0.43	29
β2-α3 interface (D chain-E chain)	-3.99	0.41	42
β2-β2 interface (C chain-D chain)	-3.68	0.25	29

By selecting different residues each time for α-conotoxin MII binding, the average free binding energy can be compared in Table 6. One-way ANOVA indicates the average binding energy for each set of binding sites was not significantly differ from the others (p-value >0.05) in α3-β2 binding pocket (Table 9 and Figure 21). The docking results were more energetically favorable compared to the results from Sambasivarao et al. (2013) (-2.9±0.3 kcal/mol for α3-β2 binding pocket with open C-loop state).

Table 9. The results produced by docking α-conotoxin MII to α3-β2 binding pocket. Results were recorded by choosing different selected binding sites. (Note: (-) means the residues were on the complementary subunit and (+) indicates the residues were on the primary subunit that contained the C-loop)

Selected binding sites	Average free binding energy (kcal/mol)	Standard deviation of free binding energy	Number of total retained poses
(-)D170, D171 (+)E194, E195	-4.89	0.54	46
(+)E194, E195	-5.07	0.56	29
(-)D170, D171	-4.40	0.44	35

The energy for binding α-conotoxin MII to different selected sites in the α3-β2 binding pocket of nAchRs are compared in a histogram (see below).

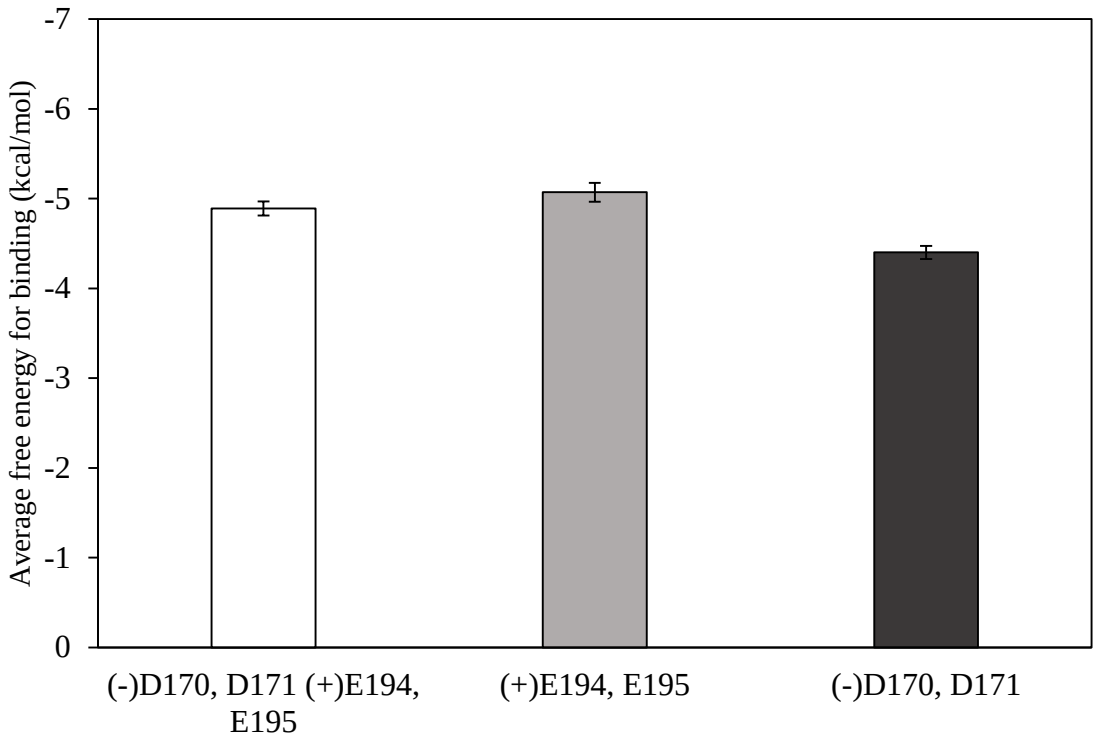

Figure 22. The average binding energy (kcal/mol) ± SEM of docking α-conotoxin MII to α3-β2 binding pockets with different combinations of selected binding sites: 1. (-)D170, D171 B. (+)E194, E195 2. (+)E194, E195 3. (-)D170, D171.

One-way ANOVA indicates the average binding energy for each set of binding sites was not significantly differ from the others (p-value >0.05) in β2-α3 binding pocket (Table 10 and Figure 22). The docking results were similar to the results from Sambasivarao et al. (2013) (-4.5±0.5 kcal/mol for β2-α3 binding pocket with open C-loop state).

Table 10. The results produced by docking mutated receptors (β2-α3 interface) with α-conotoxin MII. Results were recorded by different selected binding sites. (Note: (-) means the residues were on the complementary subunit and (+) indicates the residues were on the primary subunit that contained the C-loop)

Selected binding sites	Average free binding energy (kcal/mol)	Standard deviation of free binding energy	Number of total retained poses
(+)D192, D193, D198	-3.99	0.41	42
(+)D198	-4.05	0.42	29

The energy for binding α-conotoxin MII to different selected sites in the β2-α3 binding pocket of nAchRs are compared in a histogram (see below).

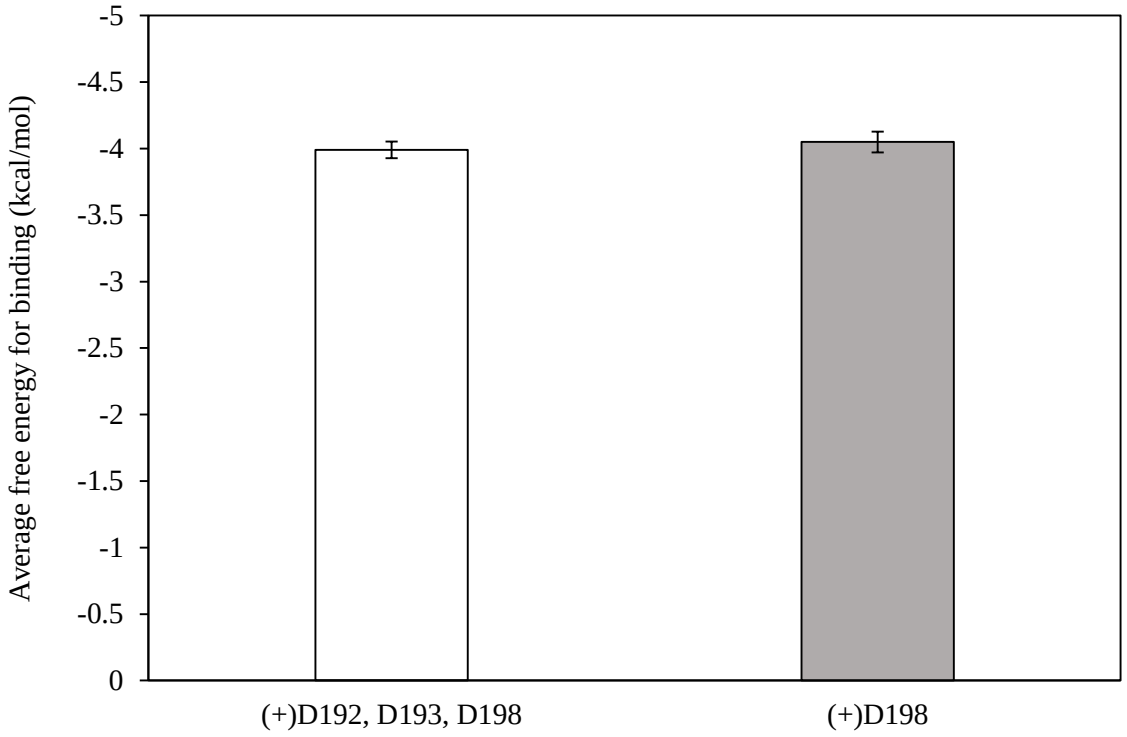

Figure 23. The average binding energy (kcal/mol) ± SEM of docking α-conotoxin MII to β2-α3 binding pockets with different combinations of selected binding sites: 1. (+)D192, D193, D198 2. (-)D198.

To investigate the effects of mutations on the C-loop in α3-β2 and β2-α3 binding pockets (C192A/C193A and D192A/D193A, respectively) may have on the binding of α-conotoxin MII, the average binding energy were compared between the wild type and mutants. Using the one-way ANOVA to compare the results of the same selected binding sites between wild type and mutant α3-β2 binding pockets in Table 11, I found that each mutant exhibit a significant difference ($p < 0.001$) compared to wild type. The α3C192A/C193A-β2 interface mutant binding pocket was more energetically favorable for α-conotoxin MII to bind than the wild type (Table 11).

Table 11. The results are compared by docking α-conotoxin MII to wild type (α3-β2) and α3C192A/C193A-β2 interface with selected all four residues ((-)D170, D171, (+)E194, E195). (Note: (-) means the residues were on the complementary subunit and (+) indicates the residues were on the primary subunit that contained the C-loop).

Selected binding sites	Average free binding energy (kcal/mol)	Standard deviation of free binding energy	Number of total retained poses
Wild type	-4.89	0.54	46
C192A/C193A	-5.42	0.45	42

The energy for binding α-conotoxin MII to wild type and mutant (C192A/C193A) nAchRs are compared in a histogram (see below).

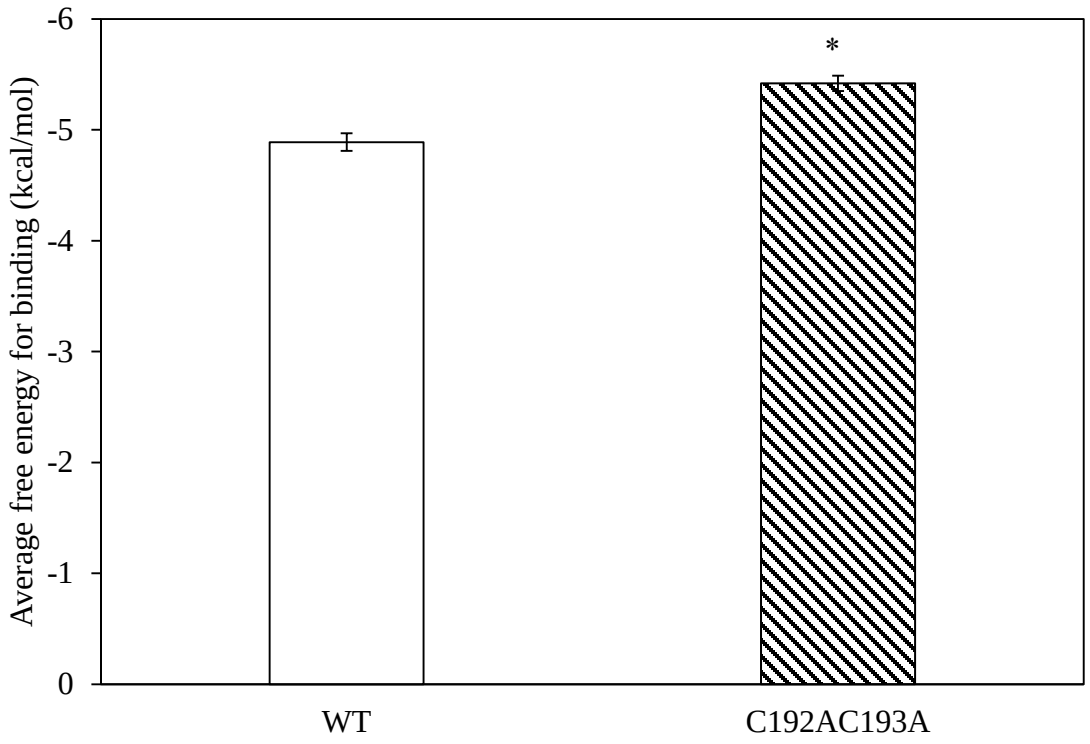

Figure 24. The average binding energy (kcal/mol) ± SEM of docking α-conotoxin MII to wild type and mutant α3-β2 binding pockets with same selected binding sites (-)D170, D171, (+)E194, E195.

A two-dimensional diagram shows how the conotoxin reside inside the wild type α3-β2 binding pocket (Figure 25), as well as a three-dimensional diagram for one of the poses of conotoxin inside the binding pocket (Figure 26). The aspartates at position 170, 171 and 199 are interacting with conotoxin as in Figure 24. Some other relevant residues inside the binding pocket that may have potential interactions with conotoxin are shown in Figure 26.

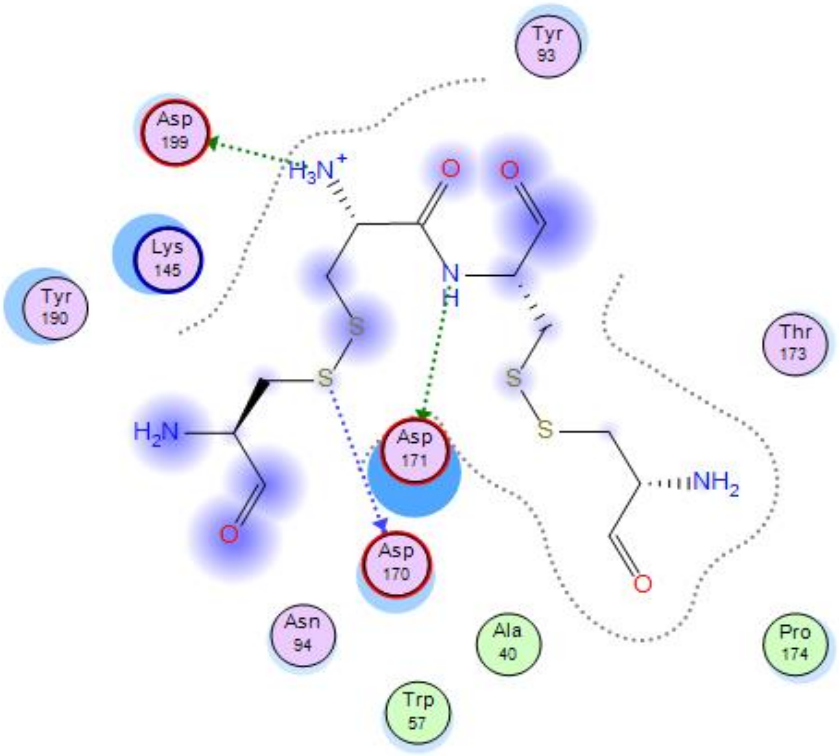

Figure 25. A 2-D diagram illustrates how α-conotoxin MII interacts with various residues in the binding pocket of α3-β2 interface. Arrows represent interactions between α-conotoxin MII and residues in the binding pocket. Image by MOE.

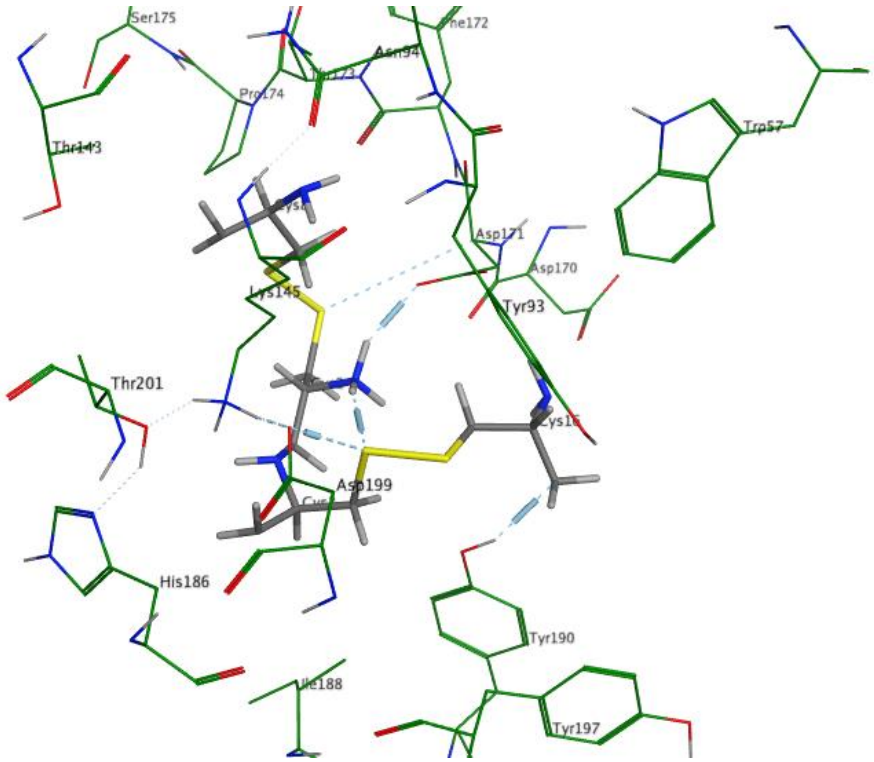

Figure 26. α-Conotoxin MII is in the binding pocket of α3-β2 interface. The residues that interact with α-conotoxin MII including W57, K145, D171 and 199, Y93 and 190.

The one-way ANOVA to compare the results of the same selected binding sites between wild type and mutant β2-α3 binding pockets in Table 12, they exhibit a significant difference ($p < 0.05$). The β2D192A/D193A-α3 interface mutant binding pocket was less energetically favorable for conotoxin to bind than the wild type (Table 12 and Figure 27).

Table 12. The results are compared by docking α-conotoxin MII to wild type (β2-α3) and α3-β2 D192A/D193A interface with selected all three residues ((+)D192A, D193A, D198). (Note: (-) means the residues were on the complementary subunit and (+) indicates the residues were on the primary subunit that contained the C-loop).

Selected binding sites	Average free binding energy (kcal/mol)	Standard deviation of free binding energy	Number of total retained poses
Wild type	-3.99	0.41	42
D192A/D193A	-3.29	1.71	36

The energy for binding α-conotoxin MII to wild type and mutant (D192A/D193A) nAchRs are compared in a histogram (see below).

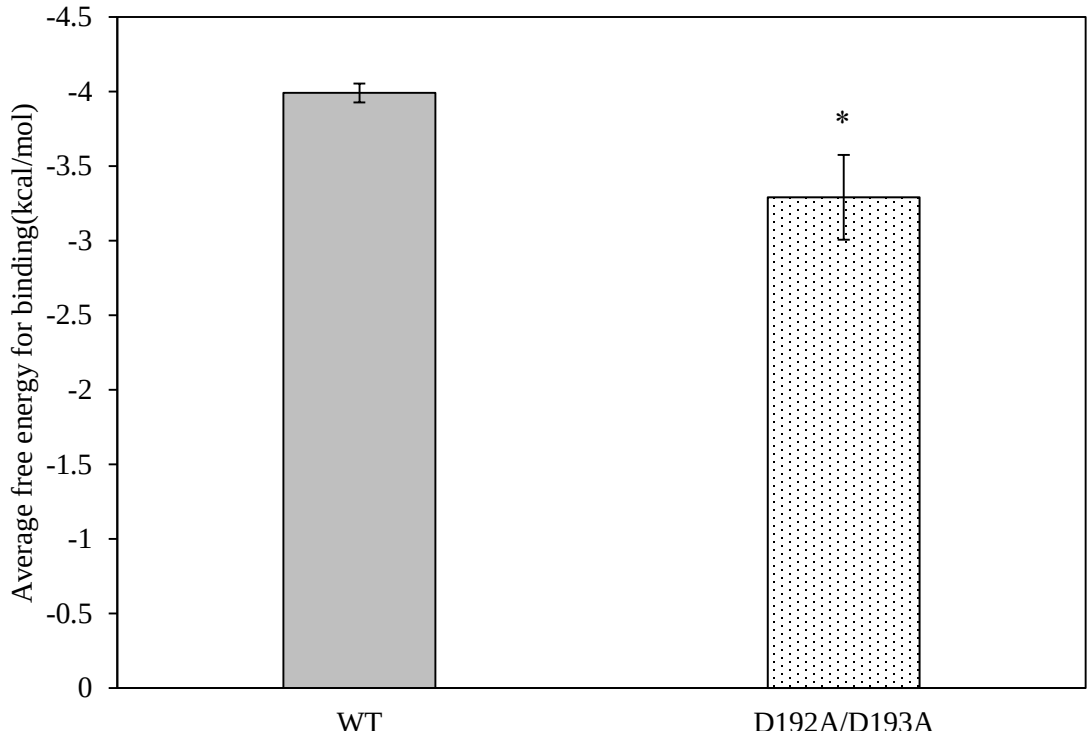

Figure 27. The average binding energy (kcal/mol) ± SEM of docking α-conotoxin MII to wild type and mutant (D192A/D193A) β2-α3 binding pockets with same selected binding sites ((+)D192A, D193A, D198).

A two-dimensional diagram shows how the conotoxin reside inside the wild type β2-α3 binding pocket (Figure 28), as well as a three-dimensional diagram for one of the poses of conotoxin inside the binding pocket (Figure 29). The residues R186, N188 and D193 are interacting with conotoxin as in Figure 28. Some other relevant residues inside the binding pocket that may have potential interactions with conotoxin are also shown in Figure 29.

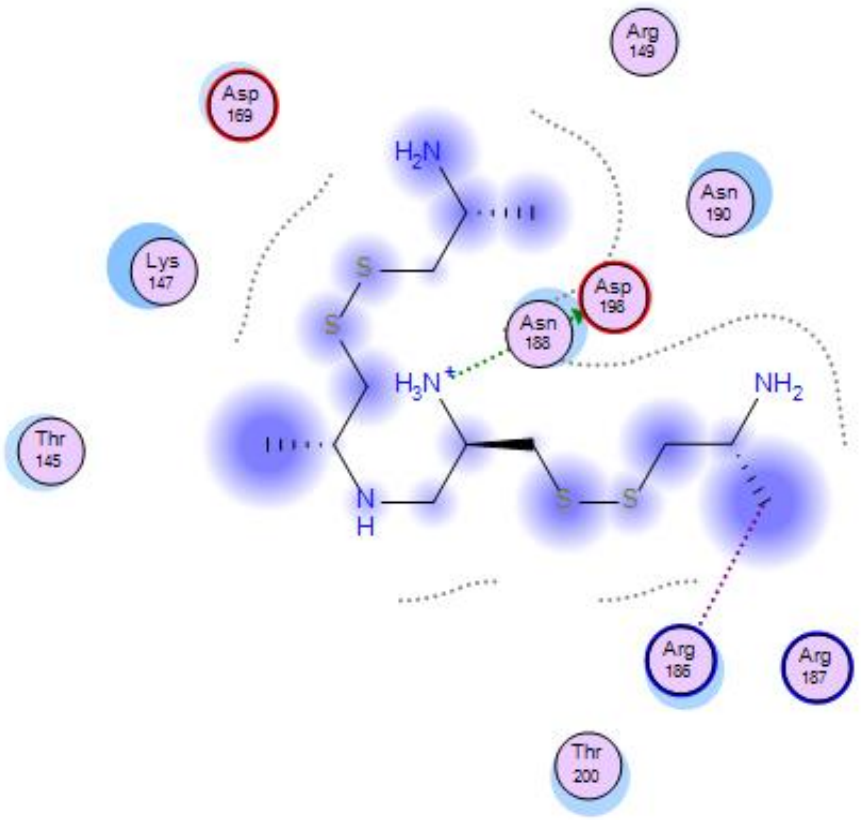

Figure 28. A 2-D diagram illustrates how α-conotoxin MII interacts with various residues in the binding pocket of β2-α3 interface. Arrows represent interactions between α-conotoxin MII and residues in the binding pocket. Image by MOE.

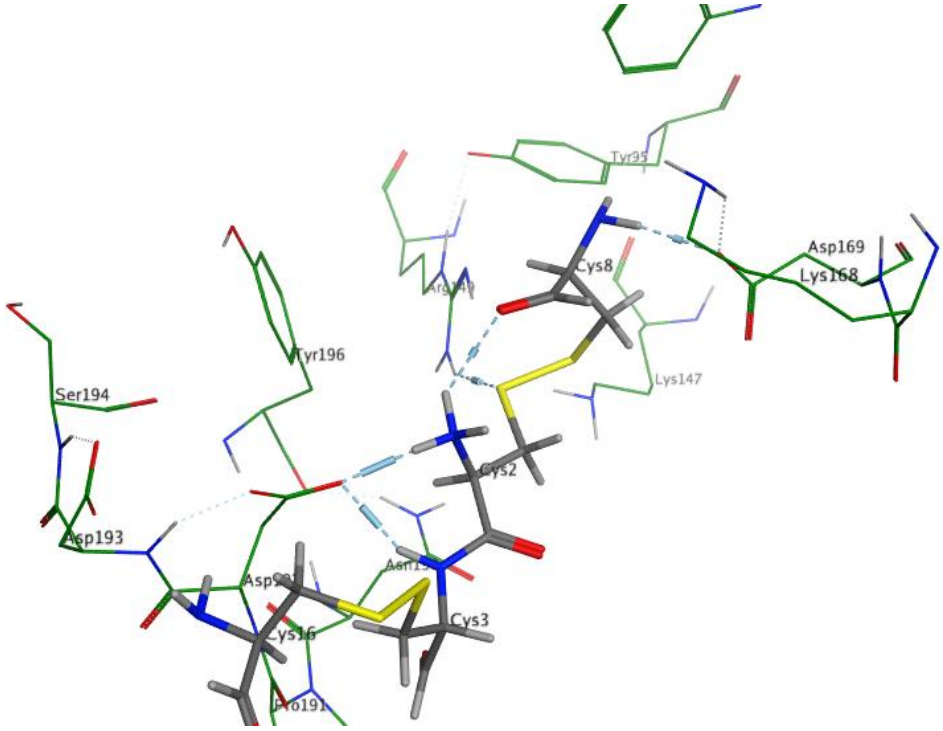

Figure 29. α-conotoxin MII is in the binding pocket of β2-α3 interface. The residues that interact with α-conotoxin MII including R149, K168, D169 and 192, Y196.

DISCUSSION

Overview of the Study

Nicotinic acetylcholine receptors (nAchRs) play important roles in the nervous system and in the periphery (Tritsch et al., 2014). These receptors are composed of different combinations of α and β subunits and exhibit a variety of function and pharmacological characteristics. Nicotinic acetylcholine receptors are often associated with neurodegenerative diseases, such as Parkinson's disease, since these receptors play an important role in regulating dopaminergic pathways in the midbrain (Purves et al., 2012) and in Alzheimer's disease, a known cholinergic disorder. This study focuses on structural aspects of the function of the α3β2 nAchRs, to shed some light on developing potential treatments for manifestations that are related to neurodegenerative diseases.

nAchRs have three conformational states: receptors are open, desensitized or closed. The open state is observed with the activated nAchR that follows the ligand binding event. Previous studies suggested that the extracellular, C-loop structure in the nAchR is a major contributor for ligand binding. Therefore, I used mutations of homologous residues in the C-loop to test the potential role of these subunits in the binding efficiency of the receptor. A better understanding of the binding determinants for this receptor will provide insight into the development of pharmacological strategies to offset neural disorders for which nAchRs play a role. Here, I provide interpretation of the functional and computational results and discuss one of these disorders involving nAchR dysfunction (Parkinson's disease) in more detail.

In order to understand how mutations on the C-loop may affect the binding efficiency of nAchRs, two neighboring aspartates (D192 and D193) in the C-loop of the β2 subunit as well as the homologous cysteines (C192 and C193) in the C-loop of the α3 subunit were mutated to alanine, for the α3β2 nAchR. In addition, I tested two quadruple mutations in both α3 and β2 subunits (C192A/C193A/D192A/D193A and C192A/C193A/D192C/D193C). Each of these mutations' inward sodium currents for a range of Ach concentrations were tested in functional studies by using two-electrode voltage clamp electrophysiology, in order to construct dose-response curves for acetylcholine, and their binding energies were tested in computational approaches with homology models and MOE simulations. A discussion of the results follows.

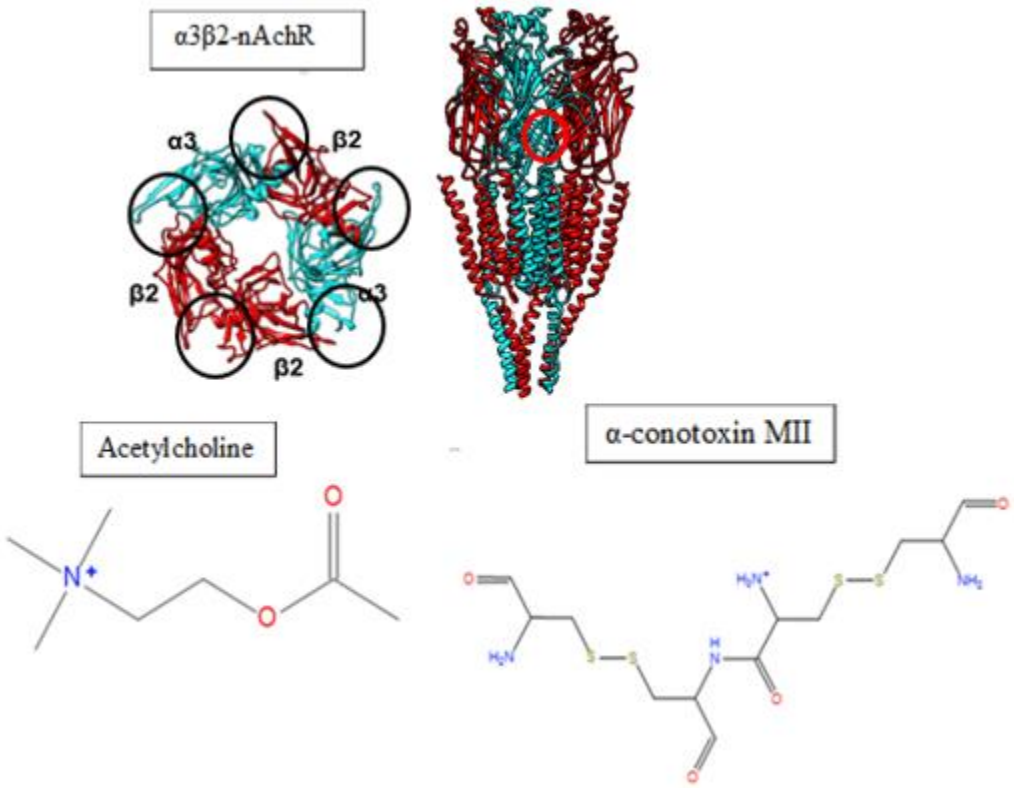

Figure 30. Top: The homology models of α3β2-nAchR that was built by using the *Aplysia californica* nicotinic acetylcholine binding protein (*Ac*-nAchBP, PDB ID: 2BR8) as the template structure. The top view (top left) shows the heteropentamer protein (red

ribbons represent β2 subunits and cyan ribbons represent α3 subunit), each black circle is the binding pocket for Ach; the central pore is in the open state to allow the flow of ions. Top right is a side view of α3β2-nAchR, where α-conotoxin MII binds slightly inferiorly to Ach as shown in red circle. Bottom left: 2-dimensional representation of acetylcholine, with the positive charged trimethyl-ammonium group and ester group. Bottom right: 2-dimensional representation of α-conotoxin MII.

Interpretation of the Functional Results

The goal for the functional experiments was to obtain dose-response curves, and compare the maximal response and the EC_{50} between wild type and mutated α3β2 nicotinic acetylcholine receptors. I found that the maximal response increased in the double cysteine to alanine mutations (C192A/C193A) in the α3 subunit and quadruple mutations (C192A/C193A/D192A/D193A) but decreased in the double aspartate to alanine mutations (D192A/D193A) in the β2 subunit compared to the wild type. The EC_{50} increased (right shift) in the double cysteine mutations, but decreased (left shift) in both the double aspartate mutations as well as in the quadruple mutations. The observed differences in EC_{50} between wild type nAchR and mutants could not be tested statistically due to the way experiments were conducted.

Based on the results, I can speculate as to the possible factors that contribute to the observed results, as well as offer possible sources of experimental limitation in the two-electrode voltage clamp work. I'll do this for comparisons of wild type and mutant channels for my findings for the effects of mutations on the maximal response, and on EC_{50}.

Maximal Response of Wild Type and Mutant Receptors

The maximal response reflects the overall efficacy of the nAchRs. The conductance of each channel of the activated receptor contributes to the overall maximal response. The term efficacy, for receptor function, was first introduced and described by Stephenson (1956), who described the relationship between receptor occupancy and its ability to produce a response. In order to initiate a response, the opening of the ion channel is required. There are two steps to open the ion channel; the first is a conformational change that occurs immediately after the ligand binds to the receptor to a higher affinity state, and is followed by the second conformational change to open the ion channel (Colquhoun, 1998). Receptors with a high efficacy can evoke the maximal response even with a low receptor occupancy. In other words, efficacy measures how efficient the receptor transit from the closed state to the active (or open) state. It is possible that mutations in the C-loop affect the efficacy of the receptor. It is unlikely, but possible, that mutations alter the conductance of the open channel when ligand is bound, but my experiments using two-electrode voltage clamp are not able to address that possibility.

The results from functional studies showed that the double cysteine mutations (C192A/C193A) in the α3 subunit as well as the quadruple mutations (C192A/C193A/D192A/D193A) had larger responses to 1 mM Ach than did the wild type, whereas the double aspartate mutations (D192A/D193A) in the β2 subunit had a lesser response (Table 1). The efficacy of the receptor increased when the two cysteines (C192 and C193) in the α3 subunit, or these two cysteines along with the two homologous aspartates in the α3 and β2 subunit respectively were mutated to alanine

(C192/C193/D192/D193). By mutating the cysteine to alanine in the α3 subunit, the protein cannot form the disulfide bridge between the two cysteines. Based on the results, both the double cysteine mutations (C192A/C193A) in the α3 subunit and the quadruple mutations (C192A/C193A/D192A/D193A) are more efficient of promoting the agonist-receptor complex from the closed state to the active (open) state. Therefore, my results suggest that the structure of the C-loop in the α3 subunit is dependent on an intact disulfide bridge, and this part of the C-loop functions to limit the availability and binding of Ach to the binding pocket.

However, the efficacy of the nAchR reduced when the two aspartates (D192 and D193) in the β2 subunit were mutated to alanine. This result suggests that these negatively charged residues are important in providing availability of Ach to the binding pocket. The side chain of alanine in the mutant β2 subunit was shorter and non-charged compared to aspartate, which has a longer and negatively charged side chain. It is possible that these negatively charged residues provide an electrostatic interaction with the cationic acetylcholine to promote more effective access to the binding pocket.

The differences between the wild type and mutant nAchR maximal response could be caused by experimental errors and variability, such as the speed and amount of Ach applied to each preparation. Other factors including the expression of nAchRs on the surface of cells as well as the residence time of Ach inside the binding pocket may have influenced the maximal response. While the magnitude and duration of the maximal response are mainly depending on the residence time of Ach inside the nAchR's binding pocket (Tummino and Copeland, 2008), expression of the subunits could also affect the results. For example, the expression of nAchRs on the cell surface various from one

oocyte to another, and this affects the number of occupied receptors when the same amount of Ach was given. Oocytes with lower nAchR expression would have lesser number of receptors occupied with Ach to produce lesser maximal response, and vice versa for oocytes with higher nAchR expression. It is possible that mutation in the α3 subunit increased, and mutation in the β2 subunit decreased, expression of the total nAchR to produce these results, which could be tested by using Western blot analysis.

EC_{50} of Wild Type and Mutant Receptors

The EC_{50}, the excitatory concentration that produces the half-maximal response, was the other important finding used for testing the hypotheses of this study. EC_{50} reflects the accessibility of the binding pocket in Ach binding and potency, which is a measure of the amount of agonist required for receptors to produce given effect or response. A reduced Ach accessibility into the binding pocket is reflected as higher or right shifted $EC_{50,}$ which also depends on both the affinity and efficacy of the receptor for Ach. An agonist with a low potency means it produces a half-maximal response at a high concentration. Potency is often assessed by EC_{50}: the left shifted EC_{50} indicates an increased potency and vice versa for the right shifted EC_{50}. The results showed the double cysteine mutations (C192A/C193A) in the α3 subunit had a slightly right shifted $EC_{50,}$ whereas both the double aspartate mutations (D192A/D193A) and the quadruple mutations (C192A/C193A/D192A/D193A) produced a significant left shifted EC_{50} (Table 1 and Figure 11, 12, and 13). The double aspartate mutations (D192A/D193A) decreased or left shifted the EC_{50} by two-thirds, and the quadruple mutations (C192A/C193A/D192A/D193A) decreased (left shifted) the EC_{50} by almost 25 folds. The

right shift in EC_{50} for C192A/C193A could imply the disulfide bridge promotes the binding or the accessibility of Ach in the α3 subunit; however, I also found an increased maximal response in that mutation. In contrast the finding that β2 subunit mutations (at D192/D193) produce left shifted EC_{50} could imply that two aspartates in the β2 subunit inhibit the Ach binding or accessibility by exerting a steric hindrance effect that may have limited the access of Ach. However, these mutations decrease the maximal response; thus, a correlation between shift in EC_{50} and maximal response was not observed. Finally, the significant left shift in EC_{50} of the quadruple mutations (C192A/C193A/D192A/D193A) could indicate there might be allosteric effect between the neighboring subunits that increases the efficacy of Ach binding.

The Hill slope that was generated by fitting the dose-response curve with the Hill equation is often used to infer the cooperativity of the binding of ligands to the receptor and the gating efficiency. In the case when the affinity is different for the first and consequential binding, the steepness of the Hill slope is affected by the concertedness of the conformational change of the receptor and the cooperativity of the binding. When the binding shows positive cooperativity, the Hill slope will be steeper and vice versa for the negative cooperative binding. However, in the case of the two binding events have the same affinity, the steepness of the Hill slope indicates the gating of the ion channel. The decreased Hill slope means there is less efficient in channel gating. When the occupancy of the first binding site affects the other or the binding sites are not equivalent, it adds complexity to interpret any changes in the Hill slope (Sine et al, 1990). In studies that created mutations in the binding site, the Hill slope will only be affected if the mutations change the ability for the ligand-receptor complex to change its conformation after the

first agonist is bound (Colquhoun, 1998). It is possible that my results, for which EC_{50} and maximal response were not correlated, are in part a consequence of allosteric effects between interfaces that each provide some degree of cooperativity in the binding of ligand (McIntosh et al., 2004).

Limitations of Functional Study

There were problems and limitations associated with different parts of the functional study as well as using two-electrode voltage clamp to test the hypotheses. The plateau of the dose-response curve was not obtained for some mutations tested, and therefore the accuracy of the maximal response and EC_{50} were in doubt. The sample size for the all the concentrations were not equal and a larger sample size is needed to improve the accuracy of the dose-response curves.

Two-electrode voltage clamp is whole-cell recording that measures the response of the population of receptors expressed in the oocyte. Two factors may cause error in determining the maximal response and comparing the effects of given mutations. First, it is possible that the mutated receptors desensitize with kinetics different than wild type nAchR with prolonged exposure to Ach. For example, a random percentage of receptors activate each time with Ach application. While some receptors are not yet activated, other, activated receptors may be transiting to the desensitized state, affecting the current amplitude and thus measurement of response. The maximal response only measures the overall response of the activated/desensitized receptors. If we could eliminate the desensitization, the maximal response is expected to be larger (Charlton, 2009) and more

consistent when comparing mutant and wild type receptors. For the double cysteine mutations and the quadruple mutations with larger responses than the wild type, it is possible that the mutations decreased the desensitization without affecting the efficacy of the receptors. The other factor that affects the maximal response is the efficiency of translation of mRNA, trafficking of the proteins, insertions into the membrane (Dash et al., 2014), and assembly of functional α3 and β2 subunits (Lukas et al., 1999). These may vary between one batch of oocytes and another, but more importantly could be different between the wild type and the mutants, affecting the observed results.

Future Experiments for Functional Study

To improve the functional results, larger sample size is needed or the highest concentration of Ach should be increased to obtain the plateau and EC_{50} with higher accuracy. In order to explain the effects of mutations have on ligand binding, other types of electrophysiology, such as single channel recording (see below) may be able to provide solutions to the problems discussed previously.

Single channel recording is the method that is often used to provide detailed information and the most direct insight for the kinetic properties of ion channels, such as channel activation (opening), desensitizing and closing events. These record the probability of the channel being open against the agonist concentrations (Lape et al., 2009). Single channel-recording can be used to compare the kinetics between a wild type and a mutated ligand-gated receptor, such as GABA, glycine, glutamate and nicotinic acetylcholine receptors. Outside-out patch recordings can be used to study nAchR by

exposing the external patch to the bath media with different concentrations of Ach, and measure the maximal response without being affected by desensitization (Mortensen and Smart, 2007). After the response for different Ach concentrations is conducted for numbers of receptors, a midpoint or EC_{50} can be calculated with high accuracy. To avoid the possible effects of desensitization, specific mutations might be created in the receptor to eliminate the desensitization and therefore allow a better measurement of the maximal response. Unfortunately, these mutations are not yet available. Single channel recording also eliminates the problems associated with the efficiency of translation and expression for the receptor when comparing the wild type to the mutants.

Experiments for local Ach application using a picospritzer can compare the desensitization of the wild type and mutant nAchRs. With a picospritzer, one can vary the time for Ach application, one can vary the time for Ach application, minimizing desensitization, and with repeated applications after desensitization, the percentage of the recovered nAchRs can be determined as a function as time (Engle et al., 2012). Another type of experiment would be to use a competitive antagonist to inhibit the wild type and mutants of nAchR to compare their recovery rate, therefore the effect of the mutations of interest have on desensitization can be elicited. Conotoxins can be used as competitive antagonists to inhibit the wild type and mutant nAchRs, followed by washout of the toxin and local application of Ach with picospritzer that varies in application time. The percent of recovery of the receptors can be determined as a function of time (Sambasivarao et al., 2013).

To gain insight into the residues that are in the binding pocket and the functions of the receptor in brain tissue, different types of toxins have been radiolabeled can be used

for measuring the functional receptors on the surface of cells for wild type receptor and mutants. Radiolabeled or fluorescent-labeled α-bungarotoxin and conotoxins can be used to measure the number of binding sites and the distribution of binding sites in rat brain tissues by binding to the receptors, and the radioactivity of the isotope and the intensity of fluorescent can then be detected in autoradiographs or under UV light (Campos-Caro et al., 1996; Azam and McIntosh, 2009). This approach is especially useful to localize specific receptor subtypes in brain regions, and could yield additional information about the role of α3β2 nicotinic acetylcholine receptors in dopaminergic pathways.

Interpretation of the Computational Results

The use of the homology model allowed me to visualize the 3-dimensional protein structure of α3β2 nAchR, and structural alterations were created for mutations of interest. MOE simulations provided energy outputs for docking Ach to wild type and mutated receptors that can be compared to each other, as well as to the results of functional study. During a MOE simulation, the interactions between Ach molecule and residues in the binding pocket were observed. After the double cysteines (C192/C193) in the α3 subunit were mutated to alanine, the disulfide bond between the two cysteines were broken. Compared to the side chain of cysteine, alanine has a shorter side chain. Similarly, after mutated the double aspartates (D192/D193) into alanine, the side chains were shorter and non-polar, perhaps disrupting a local electrostatic interaction between aspartates.

The Ach docking results showed the binding energy for both mutated receptors (C192A/C193A and D192A/D193A) were higher or less energetically favorable (less

exothermic) than wild type. This may indicate that the cysteines and aspartates are important for Ach binding, or they may interact with other residues in the binding pocket that are interacting with Ach. In both binding pockets (α3-β2 and β2-α3 interface), the residues that contributed to Ach binding include aromatic residues (tyrosine and tryptophan), other residues like serine, threonine and aspartate. There were cation-π interactions between the positively charged trimethyl-ammonium group of Ach molecule and the aromatic ring of these aromatic residues. The negatively charged side chain of aspartate may also interact with the positively charged trimethyl-ammonium group of Ach molecule. The hydrogen on the side chain of both serine and threonine may interact with the ester group to form hydrogen bonds.

The α-conotoxin MII docking results showed the receptor with double cysteine mutations (C192A/C193A) produced more energetically favorable binding than the wild type, whereas the double aspartate mutations (D192A/D193A) produced binding less energetically favorable than the wild type. It may indicate that the disulfide bridge between C192 and C193 has an inhibitory effect on the α-conotoxin MII binding, while the D192 and D193 promote or assist in α-conotoxin MII binding. By mutating the cysteine to alanine, the shorter side chain of alanine may facilitate the position of α-conotoxin MII within its binding pocket. My finding that mutation of D192 and D193 decreased α-conotoxin MII binding suggests that these residues are part of the binding sites for α-conotoxin MII, or favor interactions between conotoxin and other binding pocket residues. The models show that there are were charged residues, mainly negatively charged aspartates and one positively charged arginine that interact with α-conotoxin MII in the binding pocket of both interfaces. There were hydrogen bonds

between asparagine and α-conotoxin MII, and many hydrophobic interactions between the conotoxin and water in the binding pocket of both interfaces. The hydrophobic interactions are thought to stabilize the α-conotoxin MII inside the binding pocket, and D192/D193 may also provide stabilization in that manner.

Limitations of Homology Modeling and MOE Simulations

Although the computational approaches are important to investigate the structural mechanisms of protein functions, and a great number of computational experiments can be finished in a relative short amount time compared to functional experiments, there are limitations to this approach. It is important to note that the homology models and MOE simulations only can used as complement to functional studies, or for making predictions and refinements for future experiments. Conclusions about the mechanisms of protein functional based only on computation neither completely represent nor mimic the real mechanisms of the protein. For example, a limitation for the homology model is that the protein of interest is the mammalian neuronal nAchR, but the model was built by using the acetylcholine binding protein (AchBP) from *Aplysia californica* (invertebrate) as the template structure. In addition, the homology model was neither placed in any membranes, nor solvated. Since the nAchR is a transmembrane protein, its structure could be affected considerably without insertion into a membrane. Solvation may affect the interactions between the ligands (Ach or α-conotoxin MII) and residues inside the binding pocket of different interfaces. Finally, with MOE simulation, the time for the entrance of ligand is not determined. Also, the quadruple mutations cannot be tested with

MOE because it cannot perform docking in two binding pockets simultaneously and calculate the overall binding energy.

Future Study for Computational Approach

The suggested future studies should improve the current approach, and provide more methods that can the answer questions of interest better. What can be improved with the existing approach is to measure the distances between the ligand (Ach or α-conotoxin MII) and interactions within the binding pocket. This approach may provide a clear idea of specific residues in the binding pocket interacting with the ligand.

Molecular dynamics (MD) simulations would be a better but more complicated computational approach to do in the future. With MD, the protein can be inserted into a lipid-bilayer membrane, solvated and ionized prior to the simulation of docking. Then a docking simulation can be performed. This system can generate binding energy for the wild type and mutants. The advantages of using MD include it generates the entrance time for ligand, and it can run dockings at different binding sites simultaneously so I can compare the binding energy of the receptor with the quadruple mutations to the wild type. This system can even be used to learn about the effect of the multiple mutations in different binding pockets on the receptor as a whole.

Nicotinic Acetylcholine Receptors and Parkinson's disease

Nicotinic Acetylcholine receptors (nAchRs) in the nicotinic cholinergic system are often discussed in studies involved the pathogenesis of Parkinson's disease. The anatomical overlap between the dopaminergic and nicotinic cholinergic neurons, and functional interaction between the two suggest nAchRs to be a potential therapeutic target for movement disorders in Parkinson's disease (Quik et al., 2007; Quik et al., 2009). It has been proven that nicotine administration reduces the adverse side effect of L-DOPA, and therefore can be considered as a long-term management of Parkinson's disease. There are several nAchR subtypes including α4β2*, α6β2* and α7 in the striatum that are believed to be essential in modulating dopaminergic function (Quik et al., 2009). Additionally, activation of nAchRs in nicotinic cholinergic system improves cognitive declines that are often seen in Parkinson's patients (Levin et al., 2006). Disrupting the nigrostriatal dopaminergic pathway results in reduction of dopamine, which contributes to the onset of motor symptoms in Parkinson's disease.

Epidemiological studies suggest a correlation between smoking and incidence of Parkinson's disease (Quik, 2004). Nicotine administration have shown an improvement in motor symptoms with nigrostriatal damage parkinsonian animal models as well as in Parkinson's patients (Quik et al., 2009). In other words, stimulation of nAchRs improves the Parkinson-associated motor deficits. In order to understand the role of nicotinic acetylcholine receptors in Parkinson's disease, Quik et al. (2009) applied different nicotinic treatments to different nigrostriatal damage parkinsonian animal models to show the nicotinic exposure improves dopaminergic markers and motor functions in lesioned striatal animal models. nAchRs protect against nigrostriatal damage, but they cannot

restore the integrity of damaged dopaminergic neurons. To test for this, they compared dopaminergic markers before and after nicotinic treatment in Parkinsonian animal models. There was no significant improvement in the striatum of these animals.

The Neurotransmitter, Chemical Messenger, and Pathways of Dopamine

Dopamine (DA), an organic chemical compound that belongs to the catecholamine family, plays important roles in the brain and body. Its chemical precursor L-DOPA can cross the brain blood barrier to be converted into DA, which is often used as a treatment for Parkinson's disease. The two sites in the mammalian brain that have the highest concentration of dopaminergic neurons are the substantia nigra pars compacta and VTA (Tritsch et al., 2014). There are several dopamine pathways in the brain, and they are often involved in reward, motivation, alert and addiction. In the peripheral nervous system, dopamine increases vessel diameter to facilitate blood flow. Dopamine also reduces digestive tract mobility and inhibits the production of insulin and prolactin hormones (Purves et al., 2012).

Dopaminergic pathways are the neural pathways in the brain that are responsible for dopamine transmission between different regions of the brain. There are four major dopaminergic pathways in the brain: the mesolimbic pathway, the mesocortical pathway, the nigrostriatal pathway and the tuberoinfundibular pathway. In the mesolimbic pathway, dopamine is transported from the VTA in the midbrain to the nucleus accumbens in the ventral striatum (Melenka et al., 2009). This pathway is also known as the reward pathway, which is also linked to drug addiction (Blum et al., 2012). The

mesocortical pathway projects from the VTA to the frontal cortex, and it is believed to be critical in controlling emotion, cognitive function and motivation (Melenka et al., 2009). In the nigrostriatal pathway, dopaminergic projections from the substantia nigra pars compacta reach the caudate nucleus and putamen in the dorsal striatum. The SN and striatum are part of the basal ganglia motor loop, which is essential for modulating voluntary movements. When this pathway is affected in Parkinson's disease, patients exhibit movement deficits (Purves et al., 2012). The tuberoinfundibular pathway, is the dopaminergic pathway that regulates certain hormonal secretions. It projects from the hypothalamus to the anterior pituitary gland (Melenka et al., 2009).

After initial discoveries of neuronal pathways that contain dopamine, work done by different groups suggested a more important role of dopamine in physiological system. At that point, no one had fully explored the different components in the dopaminergic pathways and the interactions between those pathways and other neurons. The first evidence of dopamine receptors in the brain was demonstrated in an experiment done by Kebabian et al., (1972). Their experiment showed adenylyl cyclase in the brain can be activated by dopamine, which convinced them adenylyl cyclase may be the receptor, or related to the receptor, for dopamine. Seeman et al. (1976) investigated the sites in the brain where antipsychotic drugs bind, and they found both dopamine and haloperidol bind to a specific site. This site was then categorized into D1-like and D2-like dopamine receptors, depending on their pharmacological properties and interaction with adenylyl cyclase. With the development of molecular and biochemical techniques, more and more dopamine receptors were being discovered and identified. This knowledge

contributed to mapping the distribution of dopamine receptors in the brain, which provided more clues in understanding the dopaminergic pathways (Marsden, 2006).

Symptoms in Parkinson's disease and Dopaminergic Neurons

The understanding of the nigrostriatal dopamine pathway and the functional properties of nAchR have improved our knowledge and understanding of the etiology and pathogenesis of Parkinson's disease (PD) and other neurodegenerative diseases. Parkinson's disease is idiopathic, and along with Alzheimer's disease and Huntington's disease are well-known neurodegenerative disorders.

Parkinson's disease, as well as other neurodegenerative diseases, can be very devastating. It is an incurable progressive neurological disorder due to the spontaneous death of dopaminergic neurons in the substantia nigra pars compacta (Heisters, 2011). The death of dopaminergic neurons results in deficiency in nigrostriatal dopamine, which leads the major signs and symptoms of PD (Moore et al., 2005). The death of dopaminergic neurons causes a decreased dopamine level in the brain, with less dopamine affecting target regions and leading to physiological and behavioral manifestations of PD. These can be categorized into motor symptoms, non-motor symptoms and cognitive symptoms that vary from individual to individual, and change over the time course of disease progression.

According to the National Parkinson Foundation (http://www.parkinson.org/understanding-parkinsons/motor-symptoms), the classical behavioral manifestations of PD are motor symptoms, which including muscle rigidity,

stiffness of the trunk, arms or legs on one side or both side of the body, resting tremor that usually starts the in hands, bradykinesia, and postural instability that often can be observed when PD patients are walking. Non-motor symptoms often develop in the later stages of the disease, and they are often manifested as difficulty of swallowing, incontinence, excessive sleepiness especially during the day, declined sensory perceptions, hallucinations and depression. PD patients also sometimes experience pain in different parts of the body (Heisters, 2011). Cognitive impairment, especially dementia, is often associated with the end stage of PD. Declining cognition is thought to be not only due to the loss of dopaminergic neurons, but also due to the affected cholinergic neurons. It is believed that with the accumulation of Lewy bodies in cholinergic neurons, they will eventually go through apoptosis. This decreases the release of acetylcholine, which is a neurotransmitter that is essential for maintaining normal cognitive function and especially memory (Francis 1999).

Treatments for Parkinson's disease

The nigrostriatal pathway is well-known for its role in rewards responses, alertness, motivation and motor control (Bromberg-Martin et al., 2010). Any disruptions in the pathway could result in Parkinson's disease or other disorders, and therefore it is very important to understand the mechanisms and major players that are involved in the modulation of DA in the pathway, including synthesis, transmission and termination of DA. When the pathway is disrupted in Parkinson's disease, it results in death of dopaminergic neurons. There are multiple routes that lead to degeneration of

dopaminergic neurons, such as accumulation of ROS and Lewy bodies, improper formation of transport vesicles, activation of microglia and mitochondrial dysfunction.

Current medical treatments for Parkinson's disease are levodopa and its derivatives, but its efficacy decreases rapidly along with time. Other than a rapidly decreased efficacy, levodopa-derivative medications only reduce the symptoms rather than to stop or reverse the progression of the disease. Thus, much of the current research is focused on developing drugs that are more effective and last longer than levodopa and its derivatives. Therefore, the future direction is to develop drugs can halt or reverse the disease, or prevent the degeneration of dopaminergic neurons. The reciprocal interaction between cholinergic neurons and dopaminergic neurons modulates the release of dopamine, a possible way of enhancing the release of dopamine is through increasing the efficiency of agonist binding of nAchRs. For example, neurotoxins are used in the study of the ligand binding and channel gating mechanisms of nAchRs, and the process of developing potential treatments for Parkinson's disease because of their rapid effects and high affinity to their substrates (Dauer and Przedborski, 2003). Mutations that are close or inside the ligand binding pocket, are created to gain an insight into the binding of agonists and antagonists, and channel gating by functional experiments and computational approaches.

CONCLUSIONS

Both the functional and computational results supported the null hypotheses for Ach binding, which is no effect of C192A/C193A or D192A/D193A on Ach binding efficiency. There are neither significant difference in EC_{50} from the functional study, nor the binding energy from the computational study between the wild type and mutated nAchRs for Ach binding. However, the results for the α-conotoxin MII binding from the computational approach only supported the hypothesis that stated the D192A/D193A decreases the α-conotoxin MII binding efficiency. The mutation C192A/C193A increased the α-conotoxin MII binding efficiency based on its binding energy. At this point, there is not a firm conclusion can be made regarding of what are the factors that underlie the results. Future experiments are needed to explore this question.

REFERENCES

Albuquerque, E.; Pereira, E.; Alkondon, M.; Rogers, S. (2009) Mammalian Nicotinic Acetylcholine Receptors: From Structure to Function. *Physiol. Rev.* 89(1): 73 -120.

Attie, A.D. and Raines, R.T. (1995) Analysis of Receptor-Ligand Interactions. *J. Chem. Educ.* 72(2): 119-123.

Azam, L. and McIntosh, J.M. (2009) Alpha-conotoxins as pharmacological probes of nicotinic acetylcholine receptors. *Acta Pharmacol. Sin.* 30(6): 771-783.

Azam, L.; Winzer-Serhan, U.H.; Chen, Y.; Leslie, F.M. (2002) Expression of Neuronal Nicotinic Acetylcholine Receptor Subunit mRNAs Within Midbrain Dopamine Neurons. *J. Comp. Neurol*. 444:260-274.

Beene, D.; Price, K.; Lester, H.; Dougherty, D.; Lummis, S. (2004) Tyrosine Residues That Control Binding and Gating in the 5-Hydrotryptamine3 Receptor Revealed by Unnatural Amino Acid Mutagenesis. *J. Neurosci.* 24(41):9097-9104.

Blum, K.; Werner, T.; Carnes, S.; Carnes, P.; Bowirrat, A.; Giordano, J.; Oscar-Berman, M.; Gold, M. (2012). Sex, drugs, and rock 'n' roll: hypothesizing common mesolimbic activation as a function of reward gene polymorphisms. *J. Psychoactive Drugs* 44 (1): 38–55.

Bouthenet, M. L.; Souil, E.; Martres, M.P.; Sokoloff, P.; Giros, B.; Schwartz, J.C. (1991) Localization of dopamine D3 receptor mRNA in the rat brain using *in situ* hybridization histochemistry: comparison with dopamine D2 receptor mRNA. *Brain Res.* 564(2): 203-19.

Brodland, G.W. (2015) How Computational Models Can Help Unlock Biological Systems. *Semin. Cell Dev. Biol.* 47-48: 62-73.

Bromberg-Martin, E.; Matsumoto, M.; Hikosaka, O. (2010) Dopamine in motivational control: rewarding, aversive, and alerting. *Neuroscience*. 68(5): 815–834.

Campos-Caro, A.; Sala, S.; Balletsta, J.J.; Vicente-Agullo, F.; Criado, M.; Sala, F. (1996) A Single Residue in the M2-M3 Loop is A Major Determinant of Coupling Between Binding and Gating in Neuronal Nicotinic Receptors. *Proc. Natl. Acad. Sci. USA.* 93:6118-6123.

Changeux, J. (2012) The Nicotinic Acetylcholine Receptor: The Founding Father of the Pentameric Ligand-gated Ion Channel Superfamily. *J. Biol. Chem.* 287(48):40207-40215.

Charlton, S. (2009) Agonist efficacy and receptor desensitization: from partial truth to a fuller picture. *Brit. J. Pharmacol*. 2009(158): 165-168.

Colquhoun, D. (1998) Binding, gating, affinity and efficacy: The interpretation of structure-activity relationships for agonists and of the effects of mutating receptors. *Brit. J. Pharmacol.* 125:923-947.

Cui, C.; Booker, T.K.; Allen, R.S.; Grady, S.R.; Whiteaker, P.; Marks, M.J.; Salminen, O.; Tritto, T.; Butt, C.M.; Allen, W.;Stitzel, J.A.; McIntosh J.M.; Boulter, J.; Collins, A.C.; Heinemann, S.F. (2003) The β3 Nicotinic Receptor Subunit: A Component of α-Conotoxin MII-Binding Nicotinic Acetylcholine Receptors that Modulate Dopamine Release and Related Behaviors. *J. Neurosci.* 23(35): 11045-11053.

Czajkowski, C.; Karlin, A. (1994) Structure of the Nicotinic Receptor Acetylcholine -binding Site. *J. Biol. Chem.* 270(7): 3160-3164.

Dascal, N. (2000) Voltage Clamp Recordings from *Xenopus* Oocytes. *Curr. Protoc. Neurosci.* 6(12): 1-18.

Dash, B.; Li, M.D.; Lukas, R. (2014) Roles for N-terminal extracellular domains of nicotinic acetylcholine receptor (nAChR) β3 subunits in enhanced functional expression of mouse α6β2β3- and α6β4β3-nAChRs. *J. Biol. Chem.* 289: 28338 -28351.

Dauer W, Przedborski, S. (2003) Parkinson's Disease: Mechanisms and Models. *Neuroscience*. 39: 889-909.

Eisenhofer, G.; Kopin, I.J.; Goldstein, D.S. (2004) Catecholamine Metabolism: A Contemporary View with Implications for Physiology and Medicine. *Pharmacol. Rev*. 56:331-349.

Engle, S.; Broderick, H.; Drenan, R. (2012) Local Application of Drugs to Study Nicotinic Acetylcholine Receptor Function in Mouse Brain Slices. *J. Vis. Exp*. 68: 1-8.

Exley, R.; Cragg, S.J. (2008) Presynaptic Nicotinic Receptor: A Dynamic and Diverse Cholinergic Filter of Striatal Dopamine Neurotransmission. *Brit. J. Pharmacol*. 153(Suppl 1): S283-S297.

Francis, P.T.; Palmer, A.M.; Snape, M.; Wilcock, G.K. (1999) The cholinergic hypothesis of Alzheimer's disease: a review of progress. *J. Neurol. Neurosurg. Psychiatry* 66(2):137-47.

Gegg, M.; Schapira, A. (2011) PINK1-parkin-dependent mitophagy involves ubiquitination of mitofusins 1 and 2: Implications for Parkinson disease pathogenesis. *Autophagy* 7(2): 243–245.

Heisters, D. (2011). Parkinson's: symptoms, treatments and research. *Br. J. Nurs.* 20(9):548-54.

Hu Z, Bai L, Tizabi Y, Southerland W (2010) Computational Modeling Study of Human Nicotinic Acetylcholine Receptor for Developing New Drugs in the Treatment of Alcoholism. *Interdiscip. Sci*. 1(4):254-262.

Jones, B.E. (2005) From waking to sleeping: neuronal and chemical substrates. *Trends Pharmacol. Sci*. 26, 578-586.

Kebabian, J. W. and Calne, D. B. (1979). Multiple receptors for dopamine. *Nature* 277(5692):93- 6.

Kurosaki, T.; Fukuda, K.; Konno, T.; Mori, Y.; Tanaka, K.; Mishina, M.; Numa, S. (1987). Functional Properties of Nicotinic Acetylcholine Receptor Subunits Expressed in Various Combinations. *FEBS Lett.* 214(2): 253-258.

Lape, R.; Colquhoun, D.; Sivilotti, L. (2008) On the nature of partial agonism in the nicotinic receptor superfamily. *Nature* 454(7205): 722-727.

Levin, E.D.; McClernon F.J. and Rezvani, A.H. (2006) Nicotinic Effects on Cognitive Function: behavioral characterization, pharmacological specification, and anatomic localization. *Psychopharmacology* 184(3-4): 523-539.

Lindstrom, J.; Merlie, J.; Yogeeswaran, G. (1979) Biochemical properties of acetylcholine receptor subunits from Torpedo californica. *Biochemistry* 18, 4465-4470.

Lodish, H.; Berk, A.; Kaiser, C.A.; Krieger, M.; Bretscher, A.; Ploegh, H.; Amon, A. and Martin, K.C. Transmembrane Transport of Ions and Small Molecules. *Molecular Cell Biology*. 8th ed. New York: W.H. Freeman, 2016. 500-01. Print.

Lukas, R.; Changeux, J.; Novere, N.; Albuquerque, E.; Balfour, D.; Berg, D.; Bertrand, D.; Chiappinelli, V.; Clarke, P.; Collins, A.; Dani, J.; Grady, S.; Kellar, K.; Lindstrom, J.; Marks, M.; Quik, M.; Taylor, P.; Wonnacott, S. (1999) International Union of Pharmacology. XX. Current Status of the Nomenclature for Nicotinic Acetylcholine Receptors and Their Subunits. *Pharmacol. Rev*. 51(2): 397-400.

Malenka EJ, Nestler SE, Hyman RC (2009). Chapter 13: Higher Cognitive Function and Behavioral Control. *Molecular neuropharmacology: a foundation for clinical neuroscience* (2nd ed.). New York: McGraw-Hill Medical. p. 318.

Malenka RC, Nestler EJ, Hyman SE (2009). Chapter 10: Neural and Neuroendocrine Control of the Internal Milieu. In Sydor A, Brown RY. *Molecular Neuropharmacology: A Foundation for Clinical Neuroscience* (2nd ed.). New York: McGraw-Hill Medical. pp: 249.

Malenka RC, Nestler EJ, Hyman SE (2009). Chapter 6: Widely Projecting Systems: Monoamines, Acetylcholine, and Orexin. In Sydor A, Brown RY. *Molecular*

Neuropharmacology: A Foundation for Clinical Neuroscience (2nd ed.). New York: McGraw-Hill Medical. pp: 147–148, 154–157.

Mallipeddi, P.L.; Pedersen, S.E.; Briggs, J.M. (2013) Intonations of acetylcholine binding site residues contributing to nicotinic acetylcholine receptor gating: Role of residues Y93, Y190, K145, and D200. *J. Mol. Graph. Model.* 44: 161-167.

Masden, C. (2006) Dopamine: the rewarding years. *Brit. J. Pharmacol.* 147: 136–144.

McIntosh, J.M.; Azam, L.; Stahell, S.; Dowell, C.; Lindstrom, J.M.; Kuryatov, A.; Garrett, J.E.; Marks, M.J. and Whiteaker, P. (2004) Analogs of α-Conotoxin MII Are Selective for α6-Containing Nicotinic Acetylcholine Receptors. *Mol. Pharmacol.* 66(4): 944-952.

Mercuri, N. B.; Saiardi, A.; Bonci, A.; Picetti, R.; Calabresi, P.; Bernardi, G.; Borrelli, E. (1997) Loss of Autoreceptor Function in Dopaminergic Neurons From Dopamine D2 Receptor Deficient Mice. *Neuroscience* 79(2): 323-7.

Molinoff, P.B.; Wolfe, B.B.; Weiland, G.A. (1981) Quantitative Analysis of Drug-Receptor Interactions: II. Determination of the Properties of Receptor Subtypes. *Life Sci*. 29(5): 427-443.

Moore, D.; West, A; Dawson, V.; Dawson, T. (2005) Molecular Pathophysiology of Parkinson's Disease. *Annu. Rev. Neurosci.* 28:57–87.

Mortensen, M. and Smart, T. (2007) Single-channel recording of ligand-gated ion channel. *Nat. Protoc*. 2(11):2826-2827.

Papke, R.; Dwoskin, L.; Crooks, P.; Zhang, G.; Zhang, Z.; Mclntosh, J.M.; Stokes, C. (2008) Extending the Analysis of Nicotinic Receptor Antagonists with the Study of Alpha 6 Nicotinic Receptor Subunit Chimeras. *Neuropharmacology* 54(8): 1189-1200.

Purves, D.; Augustine, G.; Fitzpartrick, D.; Hall, W.; LaMantia, A.; White, L. (2012) Chapter 18: Modulation Movement by the Basal Ganglia. *Neuroscience* (5th ed.) Sinauer Associates, Inc. pp. 399-410.

Quik, M. (2004) Smoking, nicotine and Parkinson's disease. *Trends Neurosci.* 27(8): 561-568.

Quik, M.; Bordia, T. and O'leary, K. (2007) Nicotinic Receptors as CNS Target for Parkinson's disease. *Biochem. Pharmacol.* 74(8): 1224-1234.

Quik, M.; Huang, L.Z.; Parameswaran N.; Bordia, T.; Campos C.; Perez, X.A. (2009) Multiple Roles for Nicotine in Parkinson's disease. *Biochem. Pharmacol.* 78(7): 677-685.

Rothman, R. (1990) High affinity dopamine reuptake inhibitors as potential cocaine antagonists: A strategy for drug development. *Life Sci.* 46(20): 17-21.

Sambasivarao, S.; Roberts, J.; Bharadwaj, V.; Slingsby, J.; Rohleder, C.; Mallory, C.; Groome, J.; McDougal, O.; Maupin, C. (2013) Acetylcholine Promotes Binding of a-Conotoxin MII at a3b2 Nicotinic Acetylcholine Receptors. *ChemBioChem* 14: 1-13.

Schapira, M.; Abagyan, R.; Totrov, M. (2002) Structural Model of Nicotinic Acetylcholine Receptor Isotypes Bound to Acetylcholine and Nicotine. *BMC Struct. Biol*. 2(1):1-8.

Sine, S.M.; Claudio, T.; Sigworth, F.J. (1990) Activation of Torpedo acetylcholine receptors expressed in mouse fibroblasts: single channel current kinetics reveal distinct agonist binding affinities. *J. Gen Physiol.* 96: 395-437.

Stephenson, R.P. (1956) A Modification of Receptor Theory. *Brit. J. Pharmacol.* 1956(11): 379-392.

Stoof, J. C. and J. W. Kebabian (1981) Opposing roles for D-1 and D-2 dopamine receptors in efflux of cyclic AMP from rat neostriatum. *Nature* 294(5839): 366-8.

Tritsch, N.; Ding, J.; Sabatini, B. (2014) Dopaminergic neurons inhibit striatal output via non-canonical release of GABA. *Nature* 490(7419): 262–266.

Tummino PJ, Copeland RA (2008) Residence Time of Receptor-Ligand Complexes and Its Effect on Biological Function. *Biochemistry*. 47(20): 5481-5490.

Volz, H.; Gleiter, C. (1998) Monoamine Oxidase Inhibitors. *Drugs& Aging* 13(5): 341 -355.

Weiss, J. (1997) The Hill equation revisited: uses and misuses. *FASEB J.* 11(11): 835 -841.

Wonnacott, S.; Barik, J. (2007) Nicotinic Ach Receptors. *Tocris Bioscience Scientific Review Series*. 28: 1-18.

Zivin, J. and Waud, D. (1982) How to Analyze Binding, Enzyme and Uptake Data: The Simplest Case, A Single Phase. *Life Sci.* 30(17): 1407-1422.

APPENDIX

Table A. Results from two-electrode voltage clamp study comparing wild type and mutant α3β2 nAchR. Maximal response and half maximal response (EC_{50}) parameters were obtained from fits to the data using the Hill equation.

Mutations	Chi square	maximal response (μA)	EC_{50} (μM)	Average response for 1mM in amplitude (μA)	Sample size of Response for 1mM (n)
A3b2 (WT)	3.02	20.74	496.39	13.07 ±1.83	37
D192CD193C	3.82	14.71	236.56	11.84±1.59	35
C192A	5.39	20.58	279.82	12.22±1.22	34
C193A	3.26	15.72	223.16	10.21±1.06	41
C192AC193A D192CD193C	26.96	48.40	5763.95	14.67±2.61	17

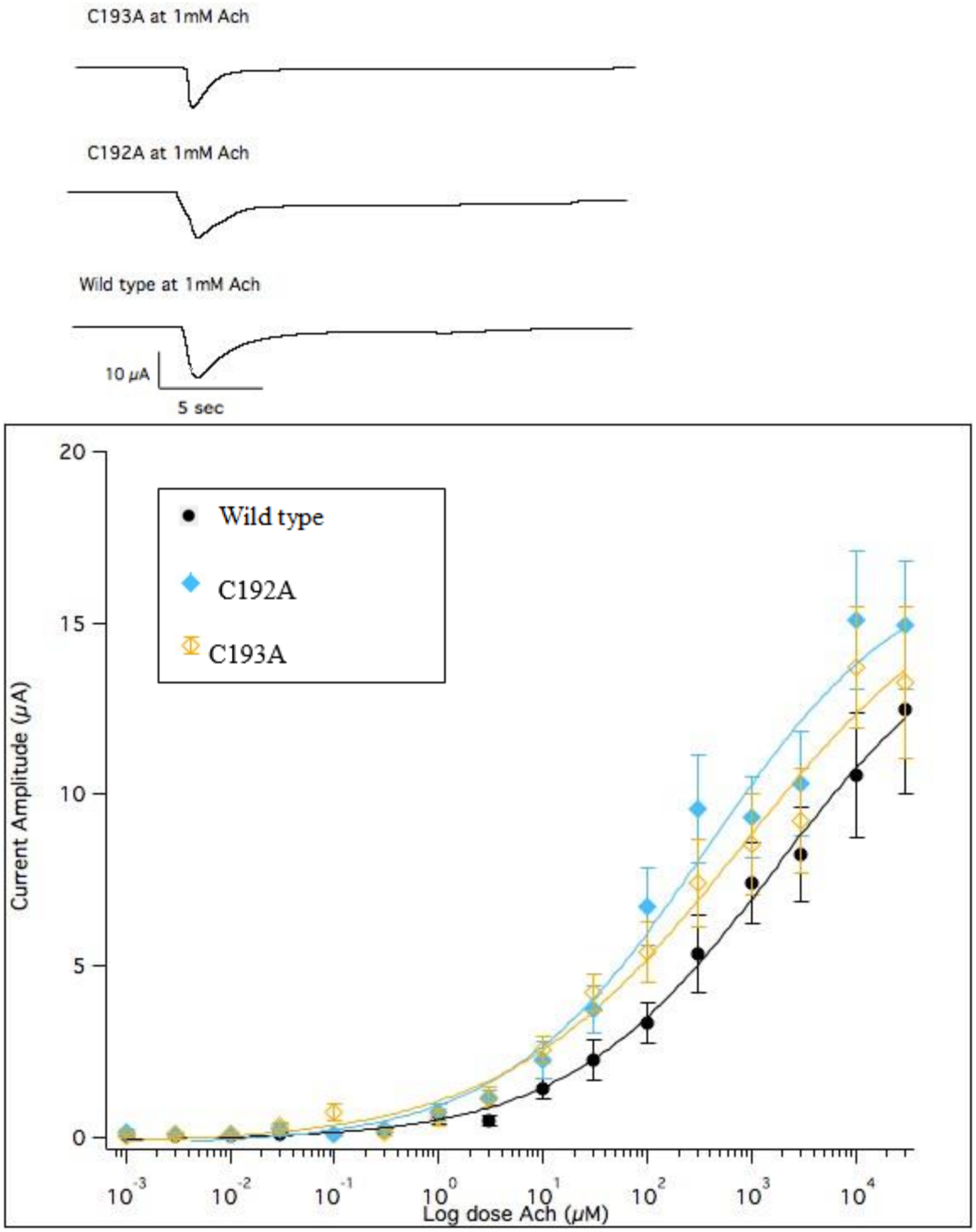

Figure A. The dose response curves of wild type, mutants C192A and C193A.

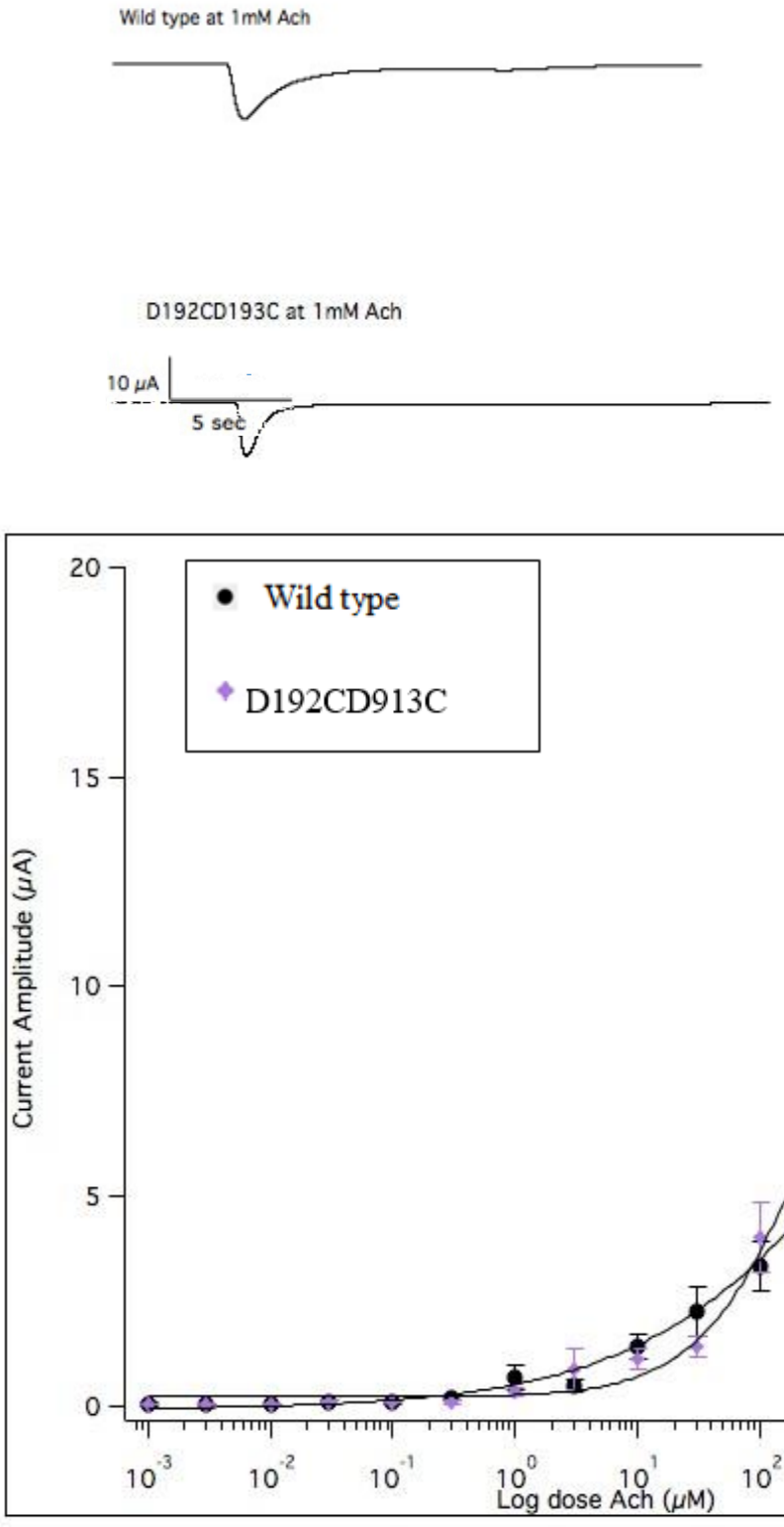

Figure B. The dose response curves of wild type, mutants D192CD193C.

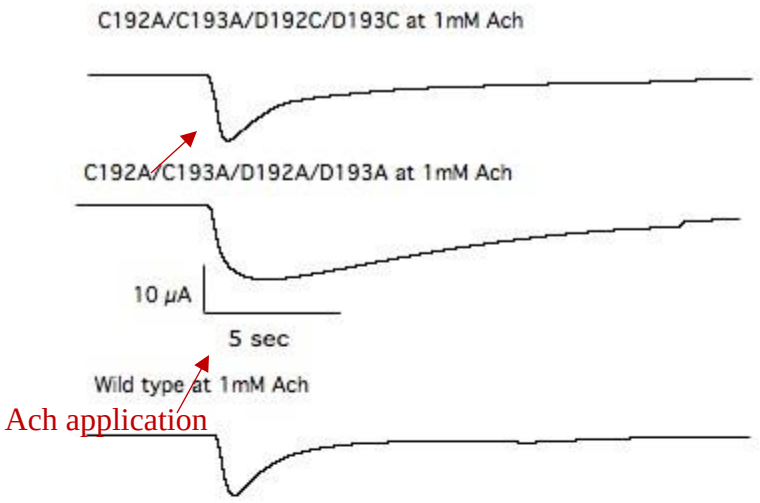
C192A/C193A/D192C/D193C at 1mM Ach
C192A/C193A/D192A/D193A at 1mM Ach
10 μA
5 sec
Wild type at 1mM Ach
Ach application

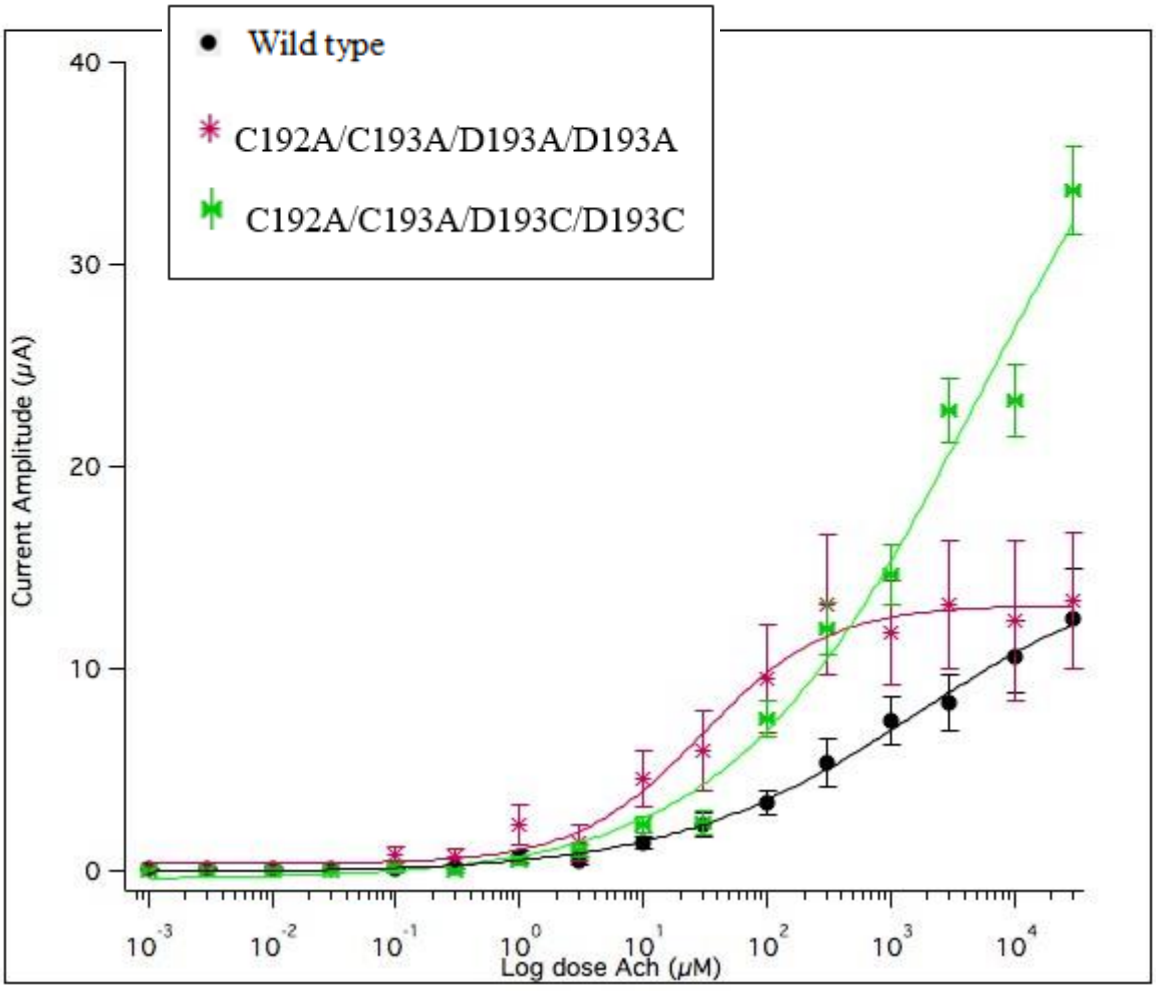
Wild type
C192A/C193A/D193A/D193A
C192A/C193A/D193C/D193C
Current Amplitude (μA)
Log dose Ach (μM)
40
30
20
10
0
10^-3
10^-2
10^-1
10^0
10^1
10^2
10^3
10^4

Figure C. The dose response curves of wild type, mutants C192A/C193A/D192C/D193C and C192A/C193A/D192A/D193A.